Measurements and Validation for the 2008/2009 Particulate Matter Study in Hong Kong

Final Report

PREPARED BY:

Dr. Judith C. Chow
Dr. John G. Watson
Mr. Steven D. Kohl
Dr. L.-W. Antony Chen

DESERT RESEARCH INSTITUTE
2215 Raggio Parkway
Reno, NV 89512
USA

PREPARED FOR:

Environmental Protection Department
The Government of Hong Kong Special Administrative Region
33/F, Revenue Tower
5 Gloucester Rd.
Wan Chai
Hong Kong

September 30, 2010

TABLE OF CONTENTS

Page

LIST OF FIGURES

LIST OF TABLES

1 INTRODUCTION

1.1 Study Objectives

The Desert Research Institute (DRI) assisted the Hong Kong Environmental Protection Department (HKEPD) in the analysis of $PM_{2.5}$ samples acquired over the course of yearlong from 12/06/2008 to 12/29/2009. The objectives of this study were to:

- Evaluate sampling and measurement methods for inorganic and organic particulate components and for gaseous precursors and end products of particle-forming atmospheric reactions.
- Determine the organic and inorganic composition of $PM_{2.5}$ and how it differs by season and proximity to different source types. Understand the atmospheric conditions causing $PM_{2.5}$ episodes.
- Based on ambient concentrations of marker compounds, source measurements performed elsewhere, and available Hong Kong emissions inventories, determine which sources are the most probable contributors to $PM_{2.5}$ in Hong Kong.
- Establish interannual variability of $PM_{2.5}$ concentration and chemical composition in Hong Kong urban and rural areas.

1.2 Background

The Hong Kong Environmental Protection Department (HKEPD) currently has not established or adopted ambient air quality standards for fine particulate matter, particles with aerodynamic diameters less than 2.5 microns ($PM_{2.5}$). Current standards in Hong Kong reflect U.S. Environmental Protection Agency (EPA) National Ambient Air Quality Standards (NAAQS) for PM_{10}.

Chemically speciated $PM_{2.5}$ and PM_{10} data from a 1998-99 pilot at Tsuen Wan, Hong Kong, showed that: 1) ~70% of PM_{10} is in the $PM_{2.5}$ fraction, 2) carbonaceous aerosol and secondary ammonium sulfate constituted a major portion of $PM_{2.5}$, 3) $PM_{2.5}$ concentrations and compositions varied over twofold between the warm and cold seasons, and 4) elevated levels of organic carbon were the main contributor to elevated $PM_{2.5}$ concentrations during winter. These findings were confirmed by two 12-month $PM_{2.5}$ studies carried out between 2000 and 2001 and then between 2004 and 2005. In addition, these 12-month studies revealed contrast between urban and rural sites in Hong Kong (Louie et al., 2005a; 2005b) as well as inter-annual variability. Since the U.S. EPA recommended three years of monitoring to determine compliance with standards, a third year of monitoring was planned.

The main objective of this report is to document $PM_{2.5}$ measurements and data validation for the third yearlong study. This data will be analyzed to characterize the composition and temporal and spatial variations of $PM_{2.5}$ concentrations. The object of this study is to: 1) establish the trend of $PM_{2.5}$ concentration and chemical composition by comparing the first-, second-, and third-year $PM_{2.5}$ measurements and 2) confirm the hypotheses regarding the formation of $PM_{2.5}$ episodes.

1.3 Technical Approach

During the sampling period from 12/06/2008 to 12/29/2009, 24-hour $PM_{2.5}$ mass

measurements were acquired every sixth day from the roadside-source-dominated Mong Kok (MK) site, the urban Tsuen Wan (TW) and Yuen Long (YL) site, and the regional background Hok Tsui (HT) site. Two Partisol particle samplers (Rupprecht & Patashnick, Albany, NY) were used at each site to obtain $PM_{2.5}$ samples on both Teflon-membrane and quartz-fiber 47-mm filters. All sampled Teflon-membrane and quartz-fiber filters were analyzed for mass by gravimetry by HKEPD's contractor and then subjected to full chemical analysis at DRI as documented in Section 2.2.

1.4 Guide to Report

This section states the background and objectives of the Particulate Matter Study in Hong Kong. Section 2 documents the ambient monitoring network and the unified database compiled from these measurements. The ambient database is assembled, validated, and documented in Section 3. Section 4 compares the first-, second-, and third-year $PM_{2.5}$ measurement results. A report summary and recommendations are provided in Section 5. The bibliography and references are assembled in Section 6.

2 SAMPLING NETWORK

2.1 Ambient Network

Twenty-four-hour $PM_{2.5}$ filter samples were taken at four sites in Hong Kong. Sampling took place every sixth day from 12/06/2008 to 12/29/2009. The ambient monitoring network shown in Figure 2-1 was designed to represent roadside (source), urban (receptor), and rural (background) areas that characterize $PM_{2.5}$ in Hong Kong. The sampling locations consisted of an urban roadside site at Mong Kok (MK), urban site at Tsuen Wan (TW) and Yuen Long (YL), and a rural regional background site at Hok Tsui (HT). Table 2-1 lists the site names, codes, locations, elevations, and a description of each site.

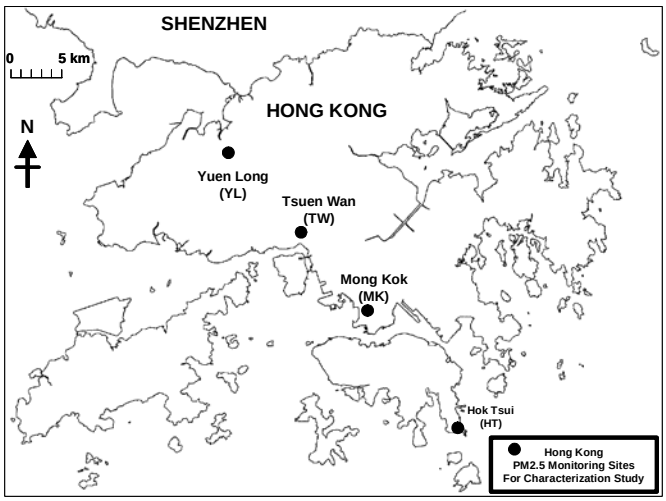

Figure 2-1. Map of the Hong Kong study area.

Table 2-1. Description of monitoring sites.

Site Name (Code) and Location	Elevation above P.D.H.K.	Site Description
Mong Kok (MK) Junction of Nathan Road and Lai Chi Kok Road	~8.5 m	An urban roadside with mixed commercial/residential area surrounded by many tall buildings.
Tsuen Wan (TW) Princess Alexandra Community Centre, 60 Tai Ho Road	~21 m	An urban, densely populated, residential site with mixed commercial and industrial developments. Located northwest of the MK site.
Yuen Long (YL) Yuen Long District Office, 269 Castle Peak Road	~31 m	A northwestern town about 15 km southwest of Shenzhen. An industrial source is located ~1 km northeast of the monitoring site.
Hok Tsui (HT) Rural location	~60 m	A rural background/transport site located about 20 km southeast of the MK site.

2.2 Ambient Particulate Measurements

Two Rupprecht & Patashnick Partisol samplers were used at each site to acquire the ambient particulate air samples. The Partisol samplers were equipped with an Andersen SA-246 size-selective inlet/WINS impactor to sample $PM_{2.5}$ at a flow rate of 16.7 L/min. At this flow rate, a nominal volume of 24.1 m^3 of ambient air would be sampled over a 24-hour period. A vacuum pump drew ambient air through the inlet and down through the filter. The flow rate was controlled by a dry gas flow meter, downstream of the sample filter, and thus not affected by filter loading.

The Partisol samplers were configured to take either a Teflon-membrane filter or a quartz-fiber filter. Lippmann (1989), Lee and Ramamurthi (1993), Watson and Chow (1993, 1994), and Chow (1995) evaluated substrates for different sampling and analyses. Based on these evaluations, the filters chosen for this study were: 1) Pall Life Sciences (Ann Arbor, MI) polymethylpentane ringed, 2.0-µm pore size, 47-mm diameter, PTFE Teflon-membrane filters (#R2PJ047) for mass and elemental analysis; and 2) Whatman (Clifton, NJ) 47-mm diameter, pre-fired QMA quartz-fiber filters (#1851-047) for carbon and ion analyses.

As shown in Figure 2-2, the Teflon-membrane filter collected particles for mass analysis by gravimetry and elemental analysis (>40 elements including Na, Mg, Al, Si, P, S, Cl, K, Ca, Ti, V, Cr, Mn, Fe, Co, Ni, Cu, Zn, Ga, As, Se, Br, Rb, Sr, Y, Zr, Mo, Pd, Ag, Cd, In, Sn, Sb, Ba, La, Au, Hg, Tl, Pb, and U) by x-ray fluorescence (Watson et al., 1999). The quartz-fiber filter, also a 47-mm diameter filter, was analyzed for mass by gravimetry, for chloride (Cl^-), nitrate (NO_3^-), and sulfate ($SO_4^=$) by ion chromatography (Chow and Watson, 1999), for ammonium (NH_4^+) by automated colorimetry, for water-soluble sodium (Na^+) and potassium (K^+) by atomic absorption spectrophotometry, and for carbon by multiple thermal evolution methods.

A major uncertainty in determining total carbon (TC) using thermal evolution methods results from differences in volatilization of certain organic compounds during sampling and storage (Fitz, 1990; Turpin et al., 1994; Chow et al., 1996). The split of organic and elemental carbon in thermal analysis, however, is even more ambiguous because it depends on temperature setpoints, temperature ramping rates, residence time at each setpoint, and combustion atmospheres, and these parameters are only empirically defined. At higher combustion temperatures, samples visibly darken as OC pyrolizes to EC in an oxygen-free environment. To overcome this problem, a laser is used to monitor changes in filter darkness during the thermal evolution process by detecting either filter reflectance (thermal/optical reflectance [TOR] method) or transmittance (thermal/optical transmittance [TOT] method).

Two analytical protocols, IMPROVE_A TOR and TOT, are used in thermal evolution analysis of TC, OC, and EC in the National Park Service's IMPROVE network since 2005. The IMPROVE network updated the TOR method in 2005 to obtain more precise temperature control and consistency of analysis atmospheres (Chow et al., 2007). This "IMPROVE_A" protocol maintains the OC-EC split but slightly alters the eight temperature-resolved carbon fractions from the original TOR method. In the IMPROVE_A protocol, total carbon is divided into eight carbon fractions as a function of temperature and oxidation environment (Chow et al., 2005; 2007). The temperature in a pure helium (He) atmosphere ramps from 25 to 140 °C (OC1), from 140 to 280 °C (OC2), from 280 to 480 °C (OC3), and

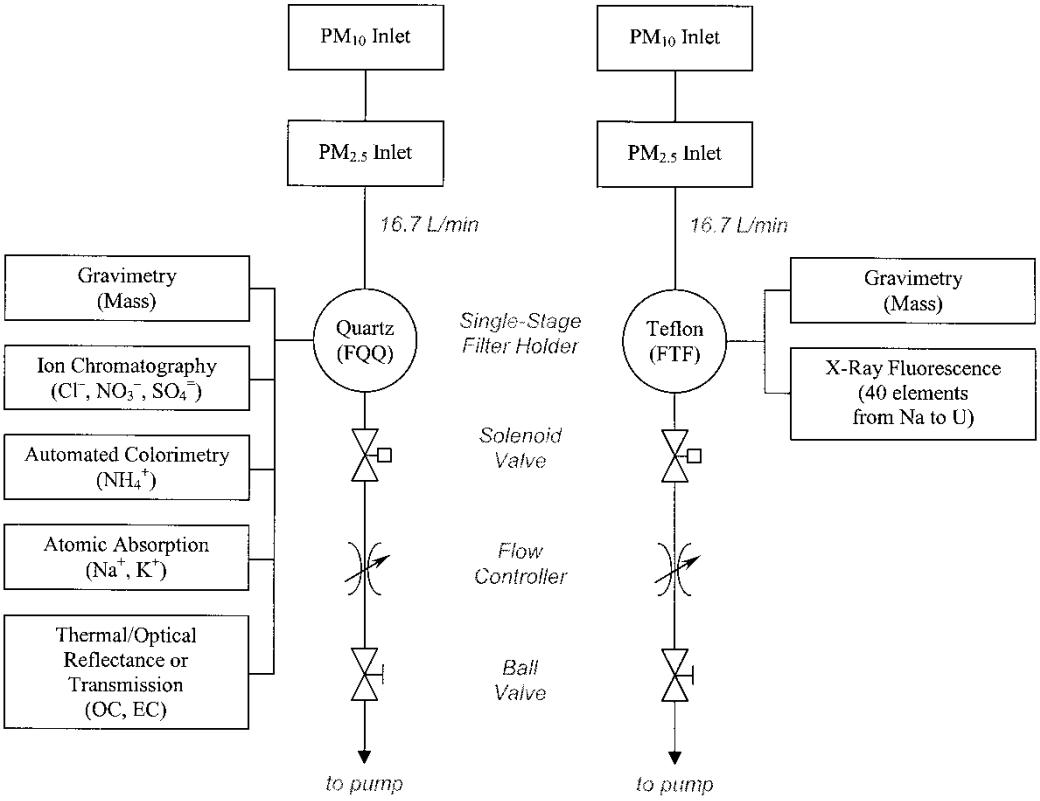

Figure 2-2. Schematic of $PM_{2.5}$ Partisol sampler configurations for the Particulate Matter Study in Hong Kong.

from 480 to 580 °C (OC4). Then, a 98% He/2% O_2 atmosphere is introduced and peaks are integrated at 580 °C (EC1), 740 °C (EC2), and 840 °C (EC3). The IMPROVE_A protocol requires the FID signal to return to baseline before advancing to the next setpoint. The fraction of pyrolyzed organic carbon (OPR or OPT) is detected in the He/O_2 atmosphere at 580 °C prior to the return of reflectance or transmittance to its original value. In the IMPROVE_A protocol, OC is defined as OC1 + OC2 + OC3 + OC4 + OPR (or OPT), and EC is defined as the difference between TC and OC. In cases laser returns to its initial value before O_2 is introduced, OC/EC split is determined when laser returns to its initial value and a negative OPR (or OPT) is reported. The carbon analyses were performed with the DRI Model 2001 analyzer (Chen et al., 2004; Chow et al., 2004; 2007). Reflectance and transmittance charring correction are both reported in Table 3-1.

The Partisol samplers were operated and maintained by HKEPD's contractor, PTC International Ltd. with support from the Hong Kong Polytechnic University (HKPU) throughout the study duration. The flow rate was periodically audited to check for any flow discrepancies and to verify instrument performance. The Teflon-membrane and quartz-fiber filters were obtained prior to sampling by the HKEPD. The HKPU was responsible for pre- and post- sampling procedures required for quality assurance and sample preservation. They were also responsible for conducting mass measurements and analysis on both filter types prior to shipping to DRI for chemical analysis.

3 DATABASE AND DATA VALIDATION

This section evaluates the precision, accuracy, and validity of the Hong Kong $PM_{2.5}$ filter data measurements. Numerous air quality studies have been conducted over the past decade, but the data obtained are often not available or applicable for data analysis and modeling because the databases lack documentation with regard to sampling and analysis methods, quality control/quality assurance procedures, accuracy specifications, precision calculations, and data validity. Lioy et al. (1980), Chow and Watson (1989), Watson and Chow (1992), and Chow and Watson (1994) summarize the requirements, limitations, and current availability of ambient and source databases in the United States. The Hong Kong $PM_{2.5}$ data set intends to meet these requirements. The data files for these studies have the following attributes:

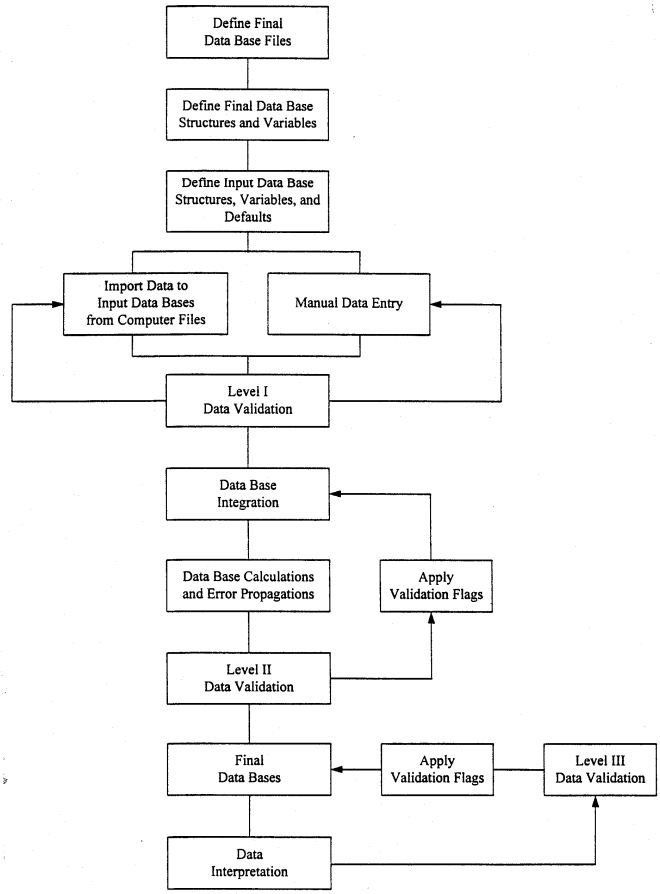

Figure 3-1. Flow diagram of the database management system.

- They contain the ambient observables needed to assess source/receptor relationships.
- They are available in a well-documented, computerized form accessible by personal computers and over the Internet.
- Measurement methods, locations, and schedules are documented.
- Precision and accuracy estimates are reported.
- Validation flags are assigned.

This section introduces the features, data structures, and contents of the Hong Kong $PM_{2.5}$ data archive. The approach that was followed to obtain the final data files is illustrated in Figure 3-1. Detailed data processing and data validation procedures are documented in Section 3.4. These data are available on floppy diskettes in Microsoft Excel (.xls) format for convenient distribution to data users. The file extension identifies the file type according to the following definitions:

- TXT = ASCII text file

- DOC = Microsoft Word document
- XLS = Microsoft Excel spreadsheet

The assembled aerosol database for filter pack measurements taken during the study is fully described in the file "HKEPD Field Names.xls" (see Table 3-1) which documents variable names, descriptions, and measurement units.

3.1 Database Structures and Features

The raw HKEPD data was processed with Microsoft FoxPro 2.6 for Windows (Microsoft Corp., 1994), a commercially available relational database management system. FoxPro can handle 256 fields of up to 4,000 characters per record and up to one billion records per file. This system can be implemented on most IBM PC-compatible desktop computers. The data base files (∗.DBF) can also be read directly into a variety of popular statistical, plotting, data base, and spreadsheet programs without having to use any specific conversion software. After processing, the final HKEPD data was converted from FoxPro to Microsoft Excel format for reporting ease and general use purposes.

In FoxPro, one of five field types (character, date, numerical, logical, or memo) was assigned to each observable. Sampling sites and particle size fractions are defined as "Character" fields, sampling dates are defined as "Date" fields, and measured data are defined as "Numeric" fields. "Logical" fields are used to represent a "yes" or "no" value applied to a variable, and "Memo" fields accommodate large blocks of textual information and are used to document the data validation results.

Data contained in different XBase files can be linked by indexing on and relating to common attributes in each file. Sampling site, sampling hour, sampling period, particle size, and sampling substrate IDs are, typically, the common fields among various data files that can be used to relate data in one file to the corresponding data in another file. To assemble the final data files, information was merged from many data files derived from field monitoring and laboratory analyses by relating information on the common fields cited above.

Table 3-1. Variable names, descriptions, and measurement units in the assembled aerosol database for filter pack measurements taken during the Particulate Matter Study in Hong Kong.

Variable Name	Description (Measurement Units)
SITE	Sampling site
DATE	Sampling date
TID	Teflon filter ID
QID	Quartz filter ID
TFFLG	Teflon field flag
QFFLG	Quartz field flag
ANIF	Anion analysis flag
N4CF	Ammonium analysis flag
NAAF	Soluble sodium analysis flag
KPAF	Soluble potassium analysis flag

Table 3-1. Continued.

Variable Name	Description (Measurement Units)
OETF	Carbon analysis flag
ELXF	XRF analysis flag
TVOC	Teflon filter volume (m3)
TVOU	Teflon filter volume uncertainty
QVOC	Quartz filter volume (m3)
QVOU	Quartz filter volume uncertainty
MSGC	Teflon Mass concentration (µg/m3)
MSGU	Teflon Mass concentration (µg/m3) uncertainty
QMSGC	QMA Mass concentration (µg/m3)
QMSGU	QMA Mass concentration (µg/m3) uncertainty
CLIC	Chloride concentration (µg/m3)
CLIU	Chloride concentration (µg/m3) uncertainty
N3IC	Nitrate concentration (µg/m3)
N3IU	Nitrate concentration (µg/m3) uncertainty
S4IC	Sulfate concentration (µg/m3)
S4IU	Sulfate concentration (µg/m3) uncertainty
N4CC	Ammonium concentration (µg/m3)
N4CU	Ammonium concentration (µg/m3) uncertainty
NAAC	Soluble Sodium concentration (µg/m3)
NAAU	Soluble Sodium concentration (µg/m3) uncertainty
KPAC	Soluble Potassium concentration (µg/m3)
KPAU	Soluble Potassium concentration (µg/m3) uncertainty
O1TC	Organic Carbon Fraction 1concentration (µg/m3)
O1TU	Organic Carbon Fraction 1 concentration (µg/m3) uncertainty
O2TC	Organic Carbon Fraction 2 concentration (µg/m3)
O2TU	Organic Carbon Fraction 2 concentration (µg/m3) uncertainty
O3TC	Organic Carbon Fraction 3 concentration (µg/m3)
O3TU	Organic Carbon Fraction 3 concentration (µg/m3) uncertainty
O4TC	Organic Carbon Fraction 4 concentration (µg/m3)
O4TU	Organic Carbon Fraction 4 concentration (µg/m3) uncertainty
OPTTC	Pyrolyzed Organic Carbon concentration (µg/m3) based upon transmittance
OPTTU	Pyrolyzed Organic Carbon concentration (µg/m3) based upon transmittance uncertainty
OPTRC	Pyrolyzed Organic Carbon concentration (µg/m3) based upon reflectance
OPTRU	Pyrolyzed Organic Carbon concentration (µg/m3) based upon reflectance uncertainty
OCTTC	Organic Carbon concentration (µg/m3) based upon transmittance
OCTTU	Organic Carbon concentration (µg/m3) based upon transmittance uncertainty
OCTRC	Organic Carbon concentration (µg/m3) based upon reflectance
OCTRU	Organic Carbon concentration (µg/m3) based upon reflectance uncertainty
E1TC	Elemental Carbon Fraction 1 concentration (µg/m3)

Table 3-1. Continued.

Variable Name	Description (Measurement Units)
E1TU	Elemental Carbon Fraction 1 concentration (µg/m3) uncertainty
E2TC	Elemental Carbon Fraction 2 concentration (µg/m3)
E2TU	Elemental Carbon Fraction 2 concentration (µg/m3) uncertainty
E3TC	Elemental Carbon Fraction 3 concentration (µg/m3)
E3TU	Elemental Carbon Fraction 3 concentration (µg/m3) uncertainty
ECTTC	Elemental Carbon concentration (µg/m3) based upon transmittance
ECTTU	Elemental Carbon concentration (µg/m3) based upon transmittance uncertainty
ECTRC	Elemental Carbon concentration (µg/m3) based upon reflectance
ECTRU	Elemental Carbon concentration (µg/m3) based upon reflectance uncertainty
TCTC	Total Carbon concentration (µg/m3)
TCTU	Total Carbon concentration (µg/m3) uncertainty
NAXC	Sodium concentration (µg/m3) (qualitative only)
NAXU	Sodium concentration (µg/m3) uncertainty
MGXC	Magnesium concentration (µg/m3) (qualitative only)
MGXU	Magnesium concentration (µg/m3) uncertainty
ALXC	Aluminum concentration (µg/m3)
ALXU	Aluminum concentration (µg/m3) uncertainty
SIXC	Silicon concentration (µg/m3)
SIXU	Silicon concentration (µg/m3) uncertainty
PHXC	Phosphorous concentration (µg/m3)
PHXU	Phosphorous concentration (µg/m3) uncertainty
SUXC	Sulfur concentration (µg/m3)
SUXU	Sulfur concentration (µg/m3) uncertainty
CLXC	Chlorine concentration (µg/m3)
CLXU	Chlorine concentration (µg/m3) uncertainty
KPXC	Potassium concentration (µg/m3)
KPXU	Potassium concentration (µg/m3) uncertainty
CAXC	Calcium concentration (µg/m3)
CAXU	Calcium concentration (µg/m3) uncertainty
SCXC	Scandium concentration (µg/m3)
SCXU	Scandium concentration (µg/m3) uncertainty
TIXC	Titanium concentration (µg/m3)
TIXU	Titanium concentration (µg/m3) uncertainty
VAXC	Vanadium concentration (µg/m3)
VAXU	Vanadium concentration (µg/m3) uncertainty
CRXC	Chromium concentration (µg/m3)
CRXU	Chromium concentration (µg/m3) uncertainty
MNXC	Manganese concentration (µg/m3)
MNXU	Manganese concentration (µg/m3) uncertainty
FEXC	Iron concentration (µg/m3)
FEXU	Iron concentration (µg/m3) uncertainty

Table 3-1. Continued.

Variable Name	Description (Measurement Units)
COXC	Cobalt concentration (µg/m3)
COXU	Cobalt concentration (µg/m3) uncertainty
NIXC	Nickel concentration (µg/m3)
NIXU	Nickel concentration (µg/m3) uncertainty
CUXC	Copper concentration (µg/m3)
CUXU	Copper concentration (µg/m3) uncertainty
ZNXC	Zinc concentration (µg/m3)
ZNXU	Zinc concentration (µg/m3) uncertainty
GAXC	Gallium concentration (µg/m3)
GAXU	Gallium concentration (µg/m3) uncertainty
ASXC	Arsenic concentration (µg/m3)
ASXU	Arsenic concentration (µg/m3) uncertainty
SEXC	Selenium concentration (µg/m3)
SEXU	Selenium concentration (µg/m3) uncertainty
BRXC	Bromine concentration (µg/m3)
BRXU	Bromine concentration (µg/m3) uncertainty
RBXC	Rubidium concentration (µg/m3)
RBXU	Rubidium concentration (µg/m3) uncertainty
SRXC	Strontium concentration (µg/m3)
SRXU	Strontium concentration (µg/m3) uncertainty
YTXC	Yttrium concentration (µg/m3)
YTXU	Yttrium concentration (µg/m3) uncertainty
ZRXC	Zirconium concentration (µg/m3)
ZRXU	Zirconium concentration (µg/m3) uncertainty
NBXC	Niobium concentration (µg/m3)
NBXU	Niobium concentration (µg/m3) uncertainty
MOXC	Molybdenum concentration (µg/m3)
MOXU	Molybdenum concentration (µg/m3) uncertainty
PDXC	Palladium concentration (µg/m3)
PDXU	Palladium concentration (µg/m3) uncertainty
AGXC	Silver concentration (µg/m3)
AGXU	Silver concentration (µg/m3) uncertainty
CDXC	Cadmium concentration (µg/m3)
CDXU	Cadmium concentration (µg/m3) uncertainty
INXC	Indium concentration (µg/m3)
INXU	Indium concentration (µg/m3) uncertainty
SNXC	Tin concentration (µg/m3)
SNXU	Tin concentration (µg/m3) uncertainty
SBXC	Antimony concentration (µg/m3)
SBXU	Antimony concentration (µg/m3) uncertainty
CSXC	Cesium concentration (µg/m3)
CSXU	Cesium concentration (µg/m3) uncertainty

Table 3-1. Continued.

Variable Name	Description (Measurement Units)
BAXC	Barium concentration (µg/m3)
BAXU	Barium concentration (µg/m3) uncertainty
LAXC	Lanthanum concentration (µg/m3)
LAXU	Lanthanum concentration (µg/m3) uncertainty
CEXC	Cerium concentration (µg/m3)
CEXU	Cerium concentration (µg/m3) uncertainty
SMXC	Samarium concentration (µg/m3)
SMXU	Samarium concentration (µg/m3) uncertainty
EUXC	Europium concentration (µg/m3)
EUXU	Europium concentration (µg/m3) uncertainty
TBXC	Terbium concentration (µg/m3)
TBXU	Terbium concentration (µg/m3) uncertainty
HFXC	Hafnium concentration (µg/m3)
HFXU	Hafnium concentration (µg/m3) uncertainty
TAXC	Tantalum concentration (µg/m3)
TAXU	Tantalum concentration (µg/m3) uncertainty
WOXC	Wolfram concentration (µg/m3)
WOXU	Wolfram concentration (µg/m3) uncertainty
IRXC	Iridium concentration (µg/m3)
IRXU	Iridium concentration (µg/m3) uncertainty
AUXC	Gold concentration (µg/m3)
AUXU	Gold concentration (µg/m3) uncertainty
HGXC	Mercury concentration (µg/m3)
HGXU	Mercury concentration (µg/m3) uncertainty
TLXC	Thallium concentration (µg/m3)
TLXU	Thallium concentration (µg/m3) uncertainty
PBXC	Lead concentration (µg/m3)
PBXU	Lead concentration (µg/m3) uncertainty
URXC	Uranium concentration (µg/m3)
URXU	Uranium concentration (µg/m3) uncertainty

Table 3-2 lists the contents of the final data files. Each observable is identified by a field name which follows a pattern for that type of observable. For example, in the filter-based aerosol concentration file, the first two characters represent the measured species (e.g., AL for aluminum, SI for silicon, CA for calcium), the third character designates the analysis method (i.e., "G" for gravimetric weighing, "X" for x-ray fluorescence analysis, "I" for ion chromatography, "A" for atomic absorption spectrophotometry, "C" for automated colorimetry, "T" for thermal/optical carbon analysis), and the last character uses a "C" to identify a species concentration or a "U" to identify the uncertainty (i.e., precision) of the

Table 3-2. Summary of $PM_{2.5}$ data files for the Particulate Matter Study in Hong Kong.

Category	Database File	Database Description
I. DATABASE DOCUMENTATION		
	HKEPD Field Names.xls	Defines the field names, measurement units, and formats used in the ambient database
II. MASS AND CHEMICAL DATA		
	HKEPD2009- PM25.XLS	Contains 24-hour $PM_{2.5}$ mass and chemical data[a,b] collected with partisol filter samplers at three sites on every sixth day between 12/06/08 and 12/29/09.
III. DATABASE VALIDATION		
	FLDFLAGS.xls	Contains the field sampling data validation flags
	CHEMFLAG.xls	Contains the chemical analysis data validation flags

[a] Includes 51 elements (Na, Mg, Al, Si, P, S, Cl, K, Ca, ,Sc,Ti, V, Cr, Mn, Fe, Co, Ni, Cu, Zn, Ga, As, Se, Br, Rb, Sr, Y, Zr, Nb, Mo, Pd, Ag, Cd, In, Sn, Sb, Cs, Ba, La, Ce, Sm, Eu, Tb, Hf, Ta, W, Ir, Au, Hg, Tl, Pb, and U) by x-ray fluorescence.

[b] Includes chloride, nitrate, and sulfate by ion chromatography; ammonium by automated colorimetry; water-soluble sodium and potassium by atomic absorption spectrophotometry; and organic carbon, elemental carbon, eight carbon fractions (OC1, OC2, OC3, OC4, OP, EC1, EC2, and EC3) by thermal/optical reflectance following the IMPROVE_A protocol.

corresponding measurement. Each measurement method is associated with a separate validation field to document the sample validity for that method. Missing or invalidated measurements have been removed and replaced with –99. All times show the start and end of the sampling period.

3.2 Measurement and Analytical Specifications

Every measurement consists of: 1) a value; 2) a precision; 3) an accuracy; and 4) a validity (Hidy, 1985; Watson et al., 1989, 2001). The measurement methods described in Section 2 are used to obtain the value. Performance testing via regular submission of standards, blank analysis, and replicate analysis are used to estimate precision. These precisions are reported in the data files described in Section 3.1 so that they can be propagated through air quality models and used to evaluate how well different values compare with one another. The submission and evaluation of independent standards through quality audits are used to estimate accuracy. Validity applies both to the measurement method and to each measurement taken with that method. The validity of each measurement is indicated by appropriate flagging within the data base, while the validity of the methods has been evaluated in this study by tests described in Section 3.4.

3.2.1 Definitions of Measurement Attributes

The precision, accuracy, and validity of the Particulate Matter Study in Hong Kong aerosol measurements are defined as follows (Chow et al., 1993a):

- A **measurement** is an observation at a specific time and place which possesses: 1) value – the center of the measurement interval; 2) precision – the width of the measurement interval; 3) accuracy – the difference between measured and reference values; and 4) validity – the compliance with assumptions made in the measurement method.

  A **measurement method** is the combination of equipment, reagents, and procedures, which provide the value of a measurement. The full description of the measurement method requires substantial documentation. For example, two methods may use the same sampling systems and the same analysis systems. These are not identical methods, however, if one performs acceptance testing on filter media and the other does not. Seemingly minor differences between methods can result in major differences between measurement values.

- **Measurement method validity** is the identification of measurement method assumptions, the quantification of effects of deviations from those assumptions, the evaluation that deviations are within reasonable tolerances for the specific application, and the creation of procedures to quantify and minimize those deviations during a specific application.

- **Sample validation** is accomplished by procedures that identify deviations from measurement assumptions and the assignment of flags to individual measurements for potential deviations from assumptions.

- The **comparability and equivalence of sampling and analysis methods** are established by the comparison of values and precisions for the same measurement obtained by different measurement methods. Interlaboratory and intralaboratory comparisons are usually made to establish this comparability. Simultaneous measurements of the same observable are considered equivalent when more than 90% of the values differ by no more than the sum of two one-sigma precision intervals for each measurement.

- **Completeness** measures how many environmental measurements with specified values, precisions, accuracies, and validities were obtained out of the total number attainable. It measures the practicability of applying the selected measurement processes throughout the measurement period. Databases which have excellent precision, accuracy, and validity may be of little use if they contain so many missing values that data interpretation is impossible.

A total of 264 ambient samples were acquired during this study, and submitted for comprehensive chemical analyses. This resulted in about 26,000 data points, as documented in Section 3.1. All of the 264 ambient aerosol samples acquired during the study were considered valid after data validation and final review. In addition, complete chemical analysis was completed on 104 field blanks, 27 lab blanks and 48 precision check samples.

A database with numerous data points, such as the one generated from this study, requires detailed documentation of precision, accuracy, and validity of the measurements. The next section addresses the procedures followed to define these quantities and presents the results of the procedures.

3.2.2 Definitions of Measurement Precision

Measurement precisions were propagated from precisions of the volumetric measurements, the chemical composition measurements, and the field blank variability using the methods of Bevington (1969) and Watson et al. (2001). The following equations calculated the precision associated with filter-based measurements:

$$C_i = (M_i - B_i)/V \quad (3\text{-}1)$$

$$V = F \times t \quad (3\text{-}2)$$

$$B_i = \frac{1}{n}\sum_{j=1}^{n} B_{ij} \quad \text{for } B_i > \sigma_{Bi} \quad (3\text{-}3)$$

$$B_i = 0 \quad \text{for } B_i \le \sigma_{Bi} \quad (3\text{-}4)$$

$$\sigma_{Bi} = STD_{Bi} = \left[\frac{1}{n-1}\sum_{j=1}^{n}(B_{ij} - B_i)^2\right]^{1/2} \quad \text{for } STD_{Bi} > SIG_{Bi} \quad (3\text{-}5)$$

$$\sigma_{Bi} = SIG_{Bi} = \left[\frac{1}{n}\sum_{j=1}^{n}(\sigma_{Bij})^2\right]^{1/2} \quad \text{for } STD_{Bi} \le SIG_{Bi} \quad (3\text{-}6)$$

$$\sigma_{Ci} = \left[\frac{\sigma_{Mi}^2 + \sigma_{Bi}^2}{V^2} + \frac{\sigma_V^2 (M_i - B_i)^2}{V^4}\right]^{1/2} \quad (3\text{-}7)$$

$$\sigma_{RMS_i} = \left(\frac{1}{n}\sum_{j=1}^{n}\sigma_{Ci}^2\right)^{1/2} \quad (3\text{-}8)$$

$$\sigma_V/V = 0.05 \quad (3\text{-}9)$$

where:

B_i = average amount of species i on field blanks

B_{ij} = the amount of species i found on field blank j

C_i = the ambient concentration of species i

F = flow rate throughout sampling period

M_i = amount of species i on the substrate

M_{ijf} = amount of species i on sample j from original analysis

M_{ijr} = amount of species i on sample j from replicate analysis

n = total number of samples in the sum

SIG_{Bi} = the root mean square error (RMSE), the square root of the averaged sum of the squared of σ_{Bij}.

STD_{Bi} = standard deviation of the blank

σ_{Bi} = blank precision for species i

σ_{Bij} = precision of the species i found on field blank j

σ_{Ci} = propagated precision for the concentration of species i

σ_{Mi} = precision of amount of species i on the substrate

σ_{RMS_i} = root mean square precision for species i

σ_V = precision of sample volume

t = sample duration

V = volume of air sampled

Dynamic field blanks were periodically placed in each sampling system without air being drawn through them to estimate the magnitude of passive deposition for the period of time which filter packs remained in a sampler (typically 24 hours). No statistically significant inter-site differences in field blank concentrations were found for any species after removal of outliers (i.e., concentration exceeding three times the standard deviations of the field blanks). The average field blank concentrations (with outliers removed) were calculated for each species on each substrate (e.g., Teflon-membrane, quartz-fiber), irrespective of the sites.

3.2.3 Analytical Specifications

Blank precisions (σ_{Bi}) are defined as the higher value of the standard deviation of the blank measurements, STD_{Bi}, or the square root of the averaged squared uncertainties of the blank concentrations, SIG_{Bi}. If the average blank for a species was less than its precision, the blank was set to zero (as shown in Equation 3-4). Dynamic field blank concentrations in µg/filter are given in Table 3-3 for $PM_{2.5}$ samples collected during the study.

The precisions (σ_{Mi}) for x-ray fluorescence analysis were determined from counting statistics unique to each sample. Hence, the σ_{Mi} is a function of the energy-specific peak area, the background, and the area under the baseline.

As shown in Table 3-3, the standard deviation of the field blank is much more than twice its corresponding root mean square error (RMSE) for water soluble sulfate ($SO_4^=$), sodium (Na^+) and potassium (K^+). It is speculated that new QMA filters used for this ion analysis already contain varied levels of Na_2SO_4 and Na_2PO_4 and potassium salt residues. Some of the field blanks might have been contaminated as well during the passive deposition period and/or during sample changing while exposed to ambient conditions. For sulfate (and nitrate), the standard deviation of the field blanks well exceeds their average. According to Equation 3-4, field blank was not subtracted for sulfate and nitrate. The measured sulfate and nitrate concentration could be biased high due to the lack of blank subtraction. Despite blank subtraction, sodium and potassium concentrations might still be biased high as negative values from Equation 3-1 were set to zero.

Filter mass and blank mass analysis was performed by the HKEPD's contractor. Blank subtractions and calculated uncertainties were not examined by DRI and were thus not included in Table 3-3 and 3-4. The largest blank level was found for soluble sodium, with an average of 39.9 ± 17.8 µg/47-mm filter. This large standard deviation in blank samples could be due to adsorption of sodium chloride during the passive sampling period when filters were left in the sampler prior to and after sampling. The proximity of the sampling

sites to the ocean (<1 km) supports this assumption. However, a large portion (>90%) of soluble sodium cannot be balanced by measured anions (i.e., chloride, sulfate and nitrate).

Table 3-4 summarizes the analytical specifications for the 24-hour $PM_{2.5}$ measurements obtained during the study. Minimum detectable limits (MDL), root mean

Table 3-3. $PM_{2.5}$ Partisol dynamic field blank concentrations at the MK, TW, YL, and HT sites during the Particulate Matter Study in Hong Kong.

	Concentrations in µg/47-mm filter					
Species	Blank Subtracted[a] (B_i)	Blank Subtracted Precision[b] (s_{Bi})	Average Field Blank	Field Blank Std. Dev. (STD_{Bi})	Root Mean Squared Blank Precision[c] (s_{RMS})	Total No. of Blanks in Average
Teflon Mass	-	-	-	-	-	-
Quartz Mass	-	-	-	-	-	-
Chloride (Cl^-)	0.0000	0.6780	-0.8274	0.6780	0.5007	100
Nitrate (NO_3^-)	0.0000	0.8630	0.8191	0.8630	0.5001	100
Sulfate ($SO_4^=$)	0.0000	11.5818	7.9095	11.5818	0.5127	100
Ammonium ($NH4^+$)	0.6631	0.5001	0.6631	0.3331	0.5001	100
Soluble Sodium (Na^+)	39.8888	17.7921	39.8888	17.7921	0.2979	100
Soluble Potassium (K^+)	0.7877	0.7645	0.7877	0.7645	0.0387	100
IMPROVE_A Protocol						
O1TC	0.0000	0.9643	0.6213	0.9643	0.5846	100
O2TC	2.7386	1.4241	2.7386	1.4241	0.9519	100
O3TC	5.8742	2.3371	5.8742	2.1032	2.3371	100
O4TC	0.0000	0.8718	0.6417	0.8312	0.8718	100
OPTTC	0.0000	0.6219	0.0929	0.3496	0.6219	100
OPTRC	0.0000	0.6206	0.0000	0.0000	0.6206	100
OCTTC	9.9686	4.3122	9.9686	4.3122	3.2556	100
OCTRC	9.8758	4.2100	9.8758	4.2100	3.2520	100
E1TC	0.0000	0.4657	0.0984	0.3023	0.4657	100
E2TC	0.0000	0.5870	0.1728	0.3278	0.5870	100
E3TC	0.0000	0.1935	0.0042	0.0307	0.1935	100
ECTTC	0.0000	0.7376	0.1826	0.4031	0.7376	100
ECTRC	0.0000	0.7377	0.2754	0.5090	0.7377	100
TCTC	10.1512	4.5081	10.1512	4.5081	3.6567	100
Sodium (Na)	0.0000	4.4615	0.2447	1.4651	4.4615	104
Magnesium (Mg)	0.0000	1.4122	0.0319	0.3264	1.4122	104
Aluminum (Al)	0.0000	0.7412	0.0171	0.2104	0.7412	104
Silicon (Si)	0.0000	0.3719	0.0756	0.3719	0.2135	104
Phosphorus (P)	0.0000	0.1719	-0.0001	0.0168	0.1719	104
Sulfur (S)	0.0000	0.1787	-0.0699	0.1394	0.1787	104
Chlorine (Cl)	0.0000	0.0922	-0.0240	0.0922	0.0697	104
Potassium (K)	0.0000	0.0726	-0.0081	0.0395	0.0726	104
Calcium (Ca)	0.0000	0.2818	-0.0069	0.1118	0.2818	104
Scandium (Sc)	0.0000	1.6196	0.0333	0.3929	1.6196	104
Titanium (Ti)	0.0000	0.0709	-0.0039	0.0222	0.0709	104
Vanadium (V)	0.0000	0.0161	-0.0003	0.0037	0.0161	104
Chromium (Cr)	0.0000	0.0269	0.0051	0.0223	0.0269	104
Manganese (Mn)	0.0000	0.1898	0.0115	0.0257	0.1898	104
Iron (Fe)	0.0000	0.1013	-0.0162	0.1013	0.0288	104

Table 3-3. (continued)

Species	Blank Subtracted[a] (B_i)	Blank Subtracted Precision[b] (s_{Bi})	Average Field Blank	Field Blank Std. Dev. (STD_{Bi})	Root Mean Squared Blank Precision[c] (s_{RMS})	Total No. of Blanks in Average
	Concentrations in µg/47-mm filter					
Cobalt (Co)	0.0000	0.0271	0.0008	0.0041	0.0271	104
Nickel (Ni)	0.0000	0.0990	-0.0012	0.0053	0.0990	104
Copper (Cu)	0.0000	0.1514	0.0006	0.0198	0.1514	104
Zinc (Zn)	0.0000	0.1687	-0.0021	0.0281	0.1687	104
Gallium (Ga)	0.0000	0.1890	-0.0069	0.0493	0.1890	104
Arsenic (As)	0.0000	0.1679	0.0002	0.0014	0.1679	104
Selenium (Se)	0.0000	0.0329	0.0010	0.0136	0.0329	104
Bromine (Br)	0.0000	0.0335	0.0015	0.0115	0.0335	104
Rubidium (Rb)	0.0000	0.0271	0.0000	0.0096	0.0271	104
Strontium (Sr)	0.0000	0.0367	-0.0021	0.0124	0.0367	104
Yttrium (Y)	0.0000	0.0237	0.0045	0.0119	0.0237	104
Zirconium (Zr)	0.0000	0.1766	0.0029	0.0316	0.1766	104
Niobium (Nb)	0.0000	0.0619	0.0010	0.0205	0.0619	104
Molybdenum (Mo)	0.0000	0.0744	0.0016	0.0205	0.0744	104
Palladium (Pd)	0.0000	0.1125	-0.0099	0.0365	0.1125	104
Silver (Ag)	0.0000	0.1033	0.0045	0.0354	0.1033	104
Cadmium (Cd)	0.0000	0.1430	-0.0123	0.0364	0.1430	104
Indium (In)	0.0000	0.1130	-0.0041	0.0336	0.1130	104
Tin (Sn)	0.0000	0.1447	-0.0147	0.0610	0.1447	104
Antimony (Sb)	0.0000	0.2122	-0.0208	0.0861	0.2122	104
Cesium (Cs)	0.0000	0.2156	-0.0007	0.0061	0.2156	104
Barium (Ba)	0.0000	0.4636	-0.0367	0.1202	0.4636	104
Lanthanum (La)	0.0000	0.8955	0.0255	0.2638	0.8955	104
Cerium (Ce)	0.0000	0.5635	0.0169	0.1829	0.5635	104
Samarium (Sm)	0.0000	1.0864	0.0688	0.2902	1.0864	104
Europium (Eu)	0.0000	1.3647	-0.0631	0.3534	1.3647	104
Terbium (Tb)	0.0000	1.0173	0.0244	0.3768	1.0173	104
Hafnium (Hf)	0.0000	0.6145	-0.0059	0.1457	0.6145	104
Tantalum (Ta)	0.0000	0.2196	-0.0016	0.0616	0.2196	104
Wolfram (W)	0.0000	0.4704	-0.0142	0.1800	0.4704	104
Iridium (Ir)	0.0000	0.0735	-0.0068	0.0296	0.0735	104
Gold (Au)	0.0000	0.0990	-0.0018	0.0357	0.0990	104
Mercury (Hg)	0.0000	0.3526	-0.0034	0.0080	0.3526	104
Thallium (Tl)	0.0000	0.0599	0.0019	0.0185	0.0599	104
Lead (Pb)	0.0000	0.0593	0.0029	0.0247	0.0593	104
Uranium (U)	0.0000	0.0702	-0.0015	0.0285	0.0702	104

** DRI did not conduct filter mass analysis. Estimated mass precision is given.

[a] Values used in data processing. Non-zero average blank concentrations are subtracted when the average blank exceeds its standard deviation.

[b] Larger of either the analytical precision or standard deviation from the field.

[c] RMS precision is the square root of the sum of the squared uncertainties of the observations divided by the number of observations.

Table 3-4. Analytical specifications for 24-hour $PM_{2.5}$ measurements at the MK, TW, YL, and HT sites during the Particulate Matter Study in Hong Kong.

Species	Analysis Method[a]	MDL[b] ($\mu g/m^3$)	RMS[c] ($\mu g/m^3$)	LQL[d] ($\mu g/m^3$)	No. of Values[e]	No. > MDL	% > MDL	No. > LQL	% > LQL
Teflon Mass	Gravimetry	-	-	-	264	-	-	-	-
Quartz Mass	Gravimetry	-	-	-	264	-	-	-	-
Chloride (Cl^-)	IC	0.0623	0.0373	0.0844	264	203	77%	182	69%
Nonvolatilized Nitrate (NO_3^-)	IC	0.0623	0.0910	0.1074	264	264	100%	264	100%
Sulfate ($SO_4^=$)	IC	0.0623	0.3798	1.4417	264	264	100%	264	100%
Ammonium (NH_4^+)	AC	0.0623	0.0941	0.0415	264	262	99%	262	99%
Soluble Sodium (Na^+)	AAS	0.0098	0.6815	2.2148	264	183	69%	2	1%
Soluble Potassium (K^+)	AAS	0.0062	0.0296	0.0952	264	263	100%	207	78%
IMPROVE_A PROTOCOL									
O1TC	TOR	0.0021	0.1953	0.1200	264	214	81%	144	55%
O2TC	TOR	0.0535	0.3432	0.1773	264	264	100%	263	100%
O3TC	TOR	0.1606	0.2757	0.2618	264	258	98%	247	94%
O4TC	TOR	0.0054	0.2714	0.1035	264	264	100%	264	100%
OPTTC	TOT	0.0054	0.2210	0.0435	264	264	100%	264	100%
OPTRC	TOR	0.0054	0.1128	0.0000	264	166	63%	167	63%
OCTTC	TOT	0.2088	0.5376	0.5368	264	264	100%	264	100%
OCTRC	TOR	0.2088	0.4439	0.5241	264	264	100%	264	100%
E1TC	TOR	0.0016	0.4099	0.0376	264	264	100%	264	100%
E2TC	TOR	0.0016	0.0776	0.0408	264	263	100%	263	100%
E3TC	TOR	0.0016	0.0114	0.0038	264	25	9%	22	8%
ECTTC	TOT	0.0054	0.3710	0.0502	264	264	100%	264	100%
ECTRC	TOR	0.0054	0.4285	0.0634	264	264	100%	264	100%
TCTC	TOR	0.2248	0.7386	0.5612	264	264	100%	264	100%
Sodium (Na)	XRF	0.1558	0.2695	0.1824	264	260	98%	258	98%
Magnesium (Mg)	XRF	0.0471	0.0814	0.0406	264	68	26%	92	35%
Aluminum (Al)	XRF	0.0186	0.0421	0.0262	264	246	93%	230	87%
Silicon (Si)	XRF	0.0150	0.0192	0.0463	264	256	97%	237	90%
Phosphorus (P)	XRF	0.0049	0.0098	0.0021	264	61	23%	61	23%
Sulfur (S)	XRF	0.0021	0.0941	0.0174	264	264	100%	264	100%
Chlorine (Cl)	XRF	0.0020	0.0071	0.0115	264	252	95%	211	80%
Potassium (K)	XRF	0.0019	0.0112	0.0049	264	264	100%	264	100%
Calcium (Ca)	XRF	0.0030	0.0163	0.0139	264	264	100%	264	100%
Scandium (Sc)	XRF	0.0080	0.0918	0.0489	264	57	22%	2	1%
Titanium (Ti)	XRF	0.0014	0.0040	0.0028	264	246	93%	224	85%
Vanadium (V)	XRF	0.0003	0.0012	0.0005	264	264	100%	264	100%
Chromium (Cr)	XRF	0.0016	0.0015	0.0028	264	91	34%	37	14%
Manganese (Mn)	XRF	0.0035	0.0108	0.0032	264	213	81%	215	81%
Iron (Fe)	XRF	0.0032	0.0061	0.0126	264	262	99%	260	98%
Cobalt (Co)	XRF	0.0002	0.0015	0.0005	264	63	24%	18	7%
Nickel (Ni)	XRF	0.0005	0.0056	0.0007	264	259	98%	256	97%
Copper (Cu)	XRF	0.0018	0.0086	0.0025	264	241	91%	229	87%
Zinc (Zn)	XRF	0.0016	0.0106	0.0035	264	261	99%	259	98%
Gallium (Ga)	XRF	0.0053	0.0108	0.0061	264	0	0%	0	0%
Arsenic (As)	XRF	0.0006	0.0094	0.0002	264	45	17%	50	19%
Selenium (Se)	XRF	0.0012	0.0019	0.0017	264	50	19%	36	14%

Table 3-4. (continued)

Species	Analysis Method[a]	MDL[b] (μg/m^3)	RMS[c] (μg/m^3)	LQL[d] (μg/m^3)	No. of Values	No. > MDL	% > MDL	No. > LQL	% > LQL
Bromine (Br)	XRF	0.0017	0.0020	0.0014	264	245	93%	248	94%
Rubidium (Rb)	XRF	0.0011	0.0016	0.0012	264	104	39%	104	39%
Strontium (Sr)	XRF	0.0026	0.0021	0.0015	264	41	16%	126	48%
Yttrium (Y)	XRF	0.0016	0.0013	0.0015	264	7	3%	9	3%
Zirconium (Zr)	XRF	0.0042	0.0100	0.0039	264	3	1%	4	2%
Niobium (Nb)	XRF	0.0028	0.0035	0.0026	264	2	1%	2	1%
Molybdenum (Mo)	XRF	0.0027	0.0043	0.0026	264	4	2%	5	2%
Palladium (Pd)	XRF	0.0064	0.0064	0.0045	264	0	0%	5	2%
Silver (Ag)	XRF	0.0061	0.0059	0.0044	264	2	1%	6	2%
Cadmium (Cd)	XRF	0.0048	0.0082	0.0045	264	6	2%	6	2%
Indium (In)	XRF	0.0053	0.0065	0.0042	264	0	0%	2	1%
Tin (Sn)	XRF	0.0057	0.0084	0.0076	264	155	59%	130	49%
Antimony (Sb)	XRF	0.0086	0.0122	0.0107	264	4	2%	2	1%
Cesium (Cs)	XRF	0.0024	0.0126	0.0008	264	0	0%	0	0%
Barium (Ba)	XRF	0.0026	0.0265	0.0150	264	81	31%	10	4%
Lanthanum (La)	XRF	0.0018	0.0509	0.0328	264	82	31%	1	0%
Cerium (Ce)	XRF	0.0017	0.0321	0.0228	264	89	34%	0	0%
Samarium (Sm)	XRF	0.0036	0.0623	0.0361	264	94	36%	7	3%
Europium (Eu)	XRF	0.0055	0.0776	0.0440	264	64	24%	5	2%
Terbium (Tb)	XRF	0.0040	0.0582	0.0469	264	74	28%	4	2%
Hafnium (Hf)	XRF	0.0164	0.0348	0.0181	264	1	0%	0	0%
Tantalum (Ta)	XRF	0.0107	0.0127	0.0077	264	1	0%	10	4%
Wolfram (W)	XRF	0.0150	0.0269	0.0224	264	0	0%	0	0%
Iridium (Ir)	XRF	0.0049	0.0042	0.0037	264	0	0%	0	0%
Gold (Au)	XRF	0.0081	0.0056	0.0044	264	0	0%	0	0%
Mercury (Hg)	XRF	0.0040	0.0200	0.0010	264	0	0%	1	0%
Thallium (Tl)	XRF	0.0027	0.0034	0.0023	264	0	0%	0	0%
Lead (Pb)	XRF	0.0039	0.0037	0.0031	264	217	82%	221	84%
Uranium (U)	XRF	0.0068	0.0040	0.0035	264	0	0%	2	1%

[a] IC=ion chromatography. AC=automated colorimetry. AAS=atomic absorption spectrophotometry. TOR= thermal/optical reflectance. TOR= thermal/optical transmittance. XRF=x-ray fluorescence.

[b] Minimum detectable limit (MDL) is the concentration at which instrument response equals three times the standard deviation of the lab blanks concentrations. Typical sample volumes are 24.1 m^3.

[c] Root mean squared precision (RMS) is the square root of the sum of the squared uncertainties of the observations divided by the number of observations.

[d] Lower quantifiable limit (LQL) is three times the standard deviation of the field blank concentrations. LQL is expressed here in terms of mass per cubic meter after dividing by 24.1 m^3 for Partisol samplers.

squared (RMS) precisions, and lower quantifiable limits (LQL) are given. The MDL is defined as the concentration at which the instrument response equals three times the standard deviation of the response to a known concentration of zero. RMS precision is the square root of the averaged squared uncertainties. The LQL is defined as a concentration corresponding to three times the standard deviation of the dynamic field blank. The LQLs in Table 3-4 were divided by 24.1 m^3, nominal 24-hour volume, for the Partisol samplers. Actual volumes varied from sample to sample, but were typically within ±5% of the pre-set volume.

The LQLs should always be equal to or larger than the analytical MDLs because they include the standard deviation of the field blank and flow rate precision (Watson et al., 2001). This was the case for most of the chemical compounds noted in Table 3-4. This table also indicates that the RMS precisions were comparable in magnitude to the LQLs for most species.

The number of reported (nonvoid, nonmissing) concentrations for each species and the number of reported concentrations greater than the MDLs and LQLs are also summarized in Table 3-4. For the study samples, mass, ions (e.g., nonvolatilized nitrate, sulfate, ammonium, and soluble potassium), organic and elemental carbon, sulfur (S), silicon (Si), Chlorine (Cl), potassium (K), calcium (Ca), ion (Fe), and zinc (Zn) were detected (> MDL) in almost all samples (more than 95%). Chloride and soluble sodium were detected in 77% and 69% of the samples, respectively. Several transition metals (e.g., Y, Mo, Zr, Pd, Ag, Cd, In, Sb, Au, Hg, Tl, and U) were not detected in most of the samples (less than 15%). This is typical for urban and non-urban sites in most regions. Other transition metals, such as titanium (Ti), copper (Cu), arsenic (As), rubidium (Rb), strontium (Sr), tin (Sn) and, lead (Pb), were detected in 93%, 91%, 17%, 39%, 16%, 59%, and 82% of the analyzed samples. These metals were above the LQLs in 85%, 87%, 19%, 39%, 48%, 49%, and 84%, respectively. Residual-oil-related species, such as nickel (Ni) and vanadium (V), were detected in 98% and 100% of the samples, respectively. Industrial-source-related toxic species such as mercury (Hg) and cadmium (Cd) were only detected in 0% and 2% of the samples, respectively. Selenium (Se) was found above the MDL in only 19% of the samples. The maximum arsenic (As) concentration of 0.0303 $\mu g/m^3$ (YL site, 8/9/2009) is a fairly high value, being over 15 times higher than the maximum concentration measured during the 2000-01 Southern Nevada Air Quality Study (SNAQS, Green et al., 2002) in the U.S. Crustal-related species such as aluminum (Al), silicon (Si), potassium (K), calcium (Ca), and iron (Fe) were found above the MDLs in over 93% of the samples and above the LQLs in more than 87% of the samples. Motor-vehicle-related species such as bromine (Br) and lead (Pb) were detected in 93% and 82% of the samples, respectively. Chlorine was detected in over 95% of the samples.

In general, the analytical specifications imply that $PM_{2.5}$ samples acquired during the study possess adequate sample loading for chemical analysis of those species that are expected from major sources in the region. The MDLs of the selected chemical analysis methods were sufficiently low to establish valid measurements with acceptable precisions. Due to the relatively high blank levels, soluble sodium was only above the LQL in 1% of the samples. Although soluble sodium was generally detectable in the samples, it likely resulted from contamination rather than environment. Soluble potassium might also be contaminated, but to a lesser degree.

3.3 Quality Assurance

Quality control (QC) and quality auditing establish the precision, accuracy, and validity of measured values. Quality assurance integrates quality control, quality auditing, measurement method validation, and sample validation into the measurement process. The results of quality assurance are data values with specified precisions, accuracies, and validities.

QC is intended to prevent, identify, correct, and define the consequences of difficulties that might affect the precision and accuracy, and or validity of the measurements. Quality auditing consisted of systems and performance audits. The system audit should include a review of the operational and QC procedures to assess whether they were adequate for assuring valid data that met the specified levels of accuracy and precision. Quality auditing should also examine all phases of the measurement activity to determine that procedures were followed and that operators were properly trained. Performance audits should establish whether the predetermined specifications were achieved in practice. The performance audits should challenge the measurement/analysis systems with known transfer standards traceable to primary standards. Quality Control and Quality Auditing procedures were carried out by the HKEPD for the samplers and for filter mass analyses. Both system and performance audits were performed in DRI's Environmental Analysis Facility on an annual basis to assure data quality. Auditors acquired and reviewed the standard operating procedures and examined all phases of measurement activities to assure that procedures were followed and that operators were properly trained.

Field blanks were acquired and replicate analyses was performed for ~10% of all ambient samples. As previously mentioned, quality assurance audits of sample flow rates were conducted by the HKEPD throughout the study period. The audit results are not included in this report, but are available from the HKEPD. Data were submitted to three levels of data validation (Chow et al., 1994, Watson et al., 2001). Detailed data validation processes are documented in the following subsections.

3.4 Data Validation

Data acquired from the study was submitted to three data validation levels:

- Level 0 sample validation designates data as they come off the instrument. This process ascertains that the field or laboratory instrument is functioning properly.
- Level I sample validation: 1) flags samples when significant deviations from measurement assumptions have occurred, 2) verifies computer file entries against data sheets, 3) eliminates values for measurements that are known to be invalid because of instrument malfunctions, 4) replaces data from a backup data acquisition system in the event of failure of the primary system, and 5) adjusts values for quantifiable calibration or interference biases.
- Level II sample validation applies consistency tests to the assembled data based on known physical relationships between variables.
- Level III sample validation is part of the data interpretation process. The first assumption upon finding a measurement which is inconsistent with physical expectations, is that the unusual value is due to a measurement error. If, upon tracing the path of the measurement nothing unusual is found, the value can be assumed to be a valid result of an environmental cause. Unusual values are identified during the data interpretation process as: 1) extreme values, 2) values which would otherwise normally track the values of other variables in a time series, and 3) values for observables which would normally follow a qualitatively predictable spatial or temporal pattern.

Level I validation flags and comments are included with each data record in the data base as documented in Section 3.1. Level II validation tests and results are described in the following subsections. Level III data validation will not be completed until further data analysis is performed.

Level II tests evaluate the chemical data for internal consistency. In this study, Level II data validations were made for: 1) sum of chemical species versus $PM_{2.5}$ mass, 2) physical consistency, 3) anion and cation balance, and 4) reconstructed versus measured mass. Correlations and linear regression statistics were computed and scatter plots prepared to examine the data.

3.4.1 Sum of Chemical Species versus Mass

The sum of the individual chemical concentrations for $PM_{2.5}$ should be less than or equal to the corresponding gravimetrically measured mass concentrations. This sum includes chemicals quantified on the Teflon-membrane and quartz-fiber filters. Total sulfur (S), soluble chloride (Cl^-), and soluble potassium (K^+) are excluded from the sum to avoid double counting since sulfate ($SO_4^=$), chlorine (Cl), and total potassium (K) are included in the sum. Elemental sodium (Na) and magnesium (Mg) have low atomic numbers and require detailed particle size distributions in order to completely correct for particle x-ray absorption effects, so these concentrations are also excluded from the calculation. Carbon is represented by OC and EC. Measured concentrations do not account for unmeasured metal oxides in crustal material, unmeasured cations, or hydrogen and oxygen associated with organic carbon.

Figure 3-2 shows scatter plots of the $PM_{2.5}$ sum of species versus mass on Teflon filters for each of the individual sites. Statistical analysis reported in each plot includes simple linear regression models whereby error is assumed in the response variate (y-axis), and no error is assumed for the explanatory variate (x-axis). Each plot contains a solid line indicating the slope with intercept and a dashed one-to-one line. Measurement uncertainties associated with the x- and y-axes are shown for comparison. Regression statistics with mass as the independent variable (X) and sum of species as the dependent variable (Y) are also calculated. The calculated correlation coefficient and number of data points is also shown for comparison, as is the average of the ratios of Y over X. As intercepts are 1.36–3.68 $\mu g/m^3$, or 5–13% of the average measured concentrations, the ratio of Y over X is slightly higher than the regression slope.

Only 5 out of the 264 sums of species are more than the corresponding $PM_{2.5}$ mass beyond the reported measurement precisions. An excellent relationship was found between the sum of species and measured mass, with correlation coefficients (R^2) exceeding 0.97 for all the measurements and individual sites. Approximately 80–88% of the $PM_{2.5}$ mass was explained by the chemical species measured during the study.

Comparisons across individual sites were similar (Figure 3-2a, b, c, and d), with the exception of the HT background site which exhibited lower mass concentrations and an intercept coefficient much closer to zero than those for the other sites. The intercepts indicate sampling artifacts (Solomon et al., 2004; Watson et al., 2009). Due to the lack of backup filters in this study, organic sampling artifacts may not be completely corrected. The elevated intercepts at MK, TW, and YL are in part attributed to the organic sampling artifacts due to relatively high carbon concentrations at these sites. The residual sulfate contamination is expected to influence these four sites more evenly.

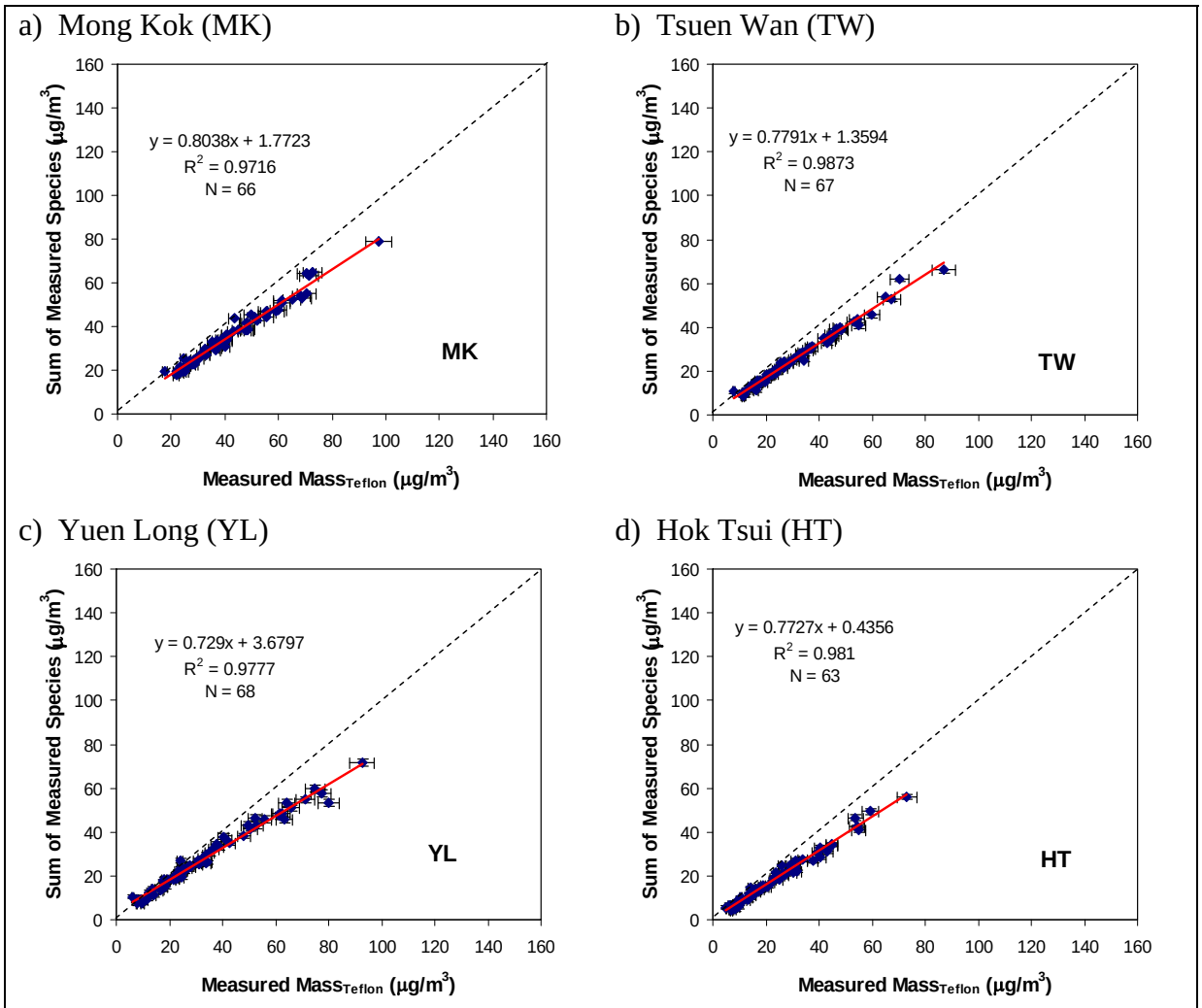

Statistics\Site	MK	TW	YL	HT	All
Slope	0.804 ± 0.017	0.779 ± 0.011	0.729 ± 0.014	0.773 ± 0.014	0.784 ± 0.007
Intercept	1.772 ± 0.780	1.359 ± 0.390	3.680 ± 0.529	0.436 ± 0.401	1.480 ± 0.282
R^2	0.972	0.987	0.978	0.981	0.977
N	66	67	68	63	264
Avg(X)	42.596	31.567	33.406	25.128	33.261
Avg(Y)	36.013	25.954	28.032	19.852	27.548
Avg(Y/X)	0.851 ± 0.060	0.836 ± 0.081	0.881 ± 0.134	0.800 ± 0.095	0.843 ± 0.100

Figure 3-2. Scatter plots of sum of species versus Teflon mass measurements from $PM_{2.5}$ data acquired at: a) the MK site; b) the TW site; c) the YL site; and d) the HT site.

3.4.2 Physical Consistency

The $PM_{2.5}$ composition in terms of chemical species concentrations measured by different chemical analysis methods was examined. Physical consistency was tested for: 1) sulfate ($SO_4^{=}$) versus total sulfur (S), 2) chloride (Cl^-) versus chlorine (Cl), and 3) soluble potassium (K^+) versus total potassium (K).

3.4.2.1 Sulfate versus Total Sulfur

Water-soluble sulfate ($SO_4^{=}$) was measured by ion chromatography (IC) analysis on quartz-fiber filters, and total sulfur (S) was measured by x-ray fluorescence (XRF) analysis on Teflon-membrane filters. The ratio of sulfate to total sulfur should equal "3" if all of the sulfur were present as soluble sulfate. Figure 3-3 shows scatter plots of sulfate versus sulfur concentrations for each of the four sites. Overall, a good correlation ($R^2 = 0.96$) was found among all $PM_{2.5}$ sulfate/sulfur measurements with a slope of 2.98 ± 0.04 and intercept of 0.44 ± 0.15 μg/m^3. This intercept is ~4% of the average measured sulfate (10.43 μg/m^3). The sulfate/sulfur ratio averages at 3.25 ± 0.81, higher than the expected values of 3, and contains variability substantially higher than those found in earlier years. This is consistent with sulfate residues observed on quartz-fiber blanks. The blank levels were not subtracted due to a large variability. Therefore, the sulfate concentrations are biased high.

High correlations ($R^2 = 0.95–0.98$) were found for $PM_{2.5}$ sulfate/sulfur comparisons among the individual sites. However, Figures 3-3a, b, c, and d show some of the data pairs fell above the three-to-one line (i.e., sulfate that is not supported by sulfur). The regression statistics give a slope ranging from 2.83 ± 0.07 to 3.12 ± 0.01 with intercept as high as 0.84 ± 0.33 μg/m^3 at the YL site). Overall, the sulfate and total sulfur comparisons in this study still support the contention that most of sulfur was present as soluble sulfate in the atmosphere, though the uncertainty in the measurements may be higher.

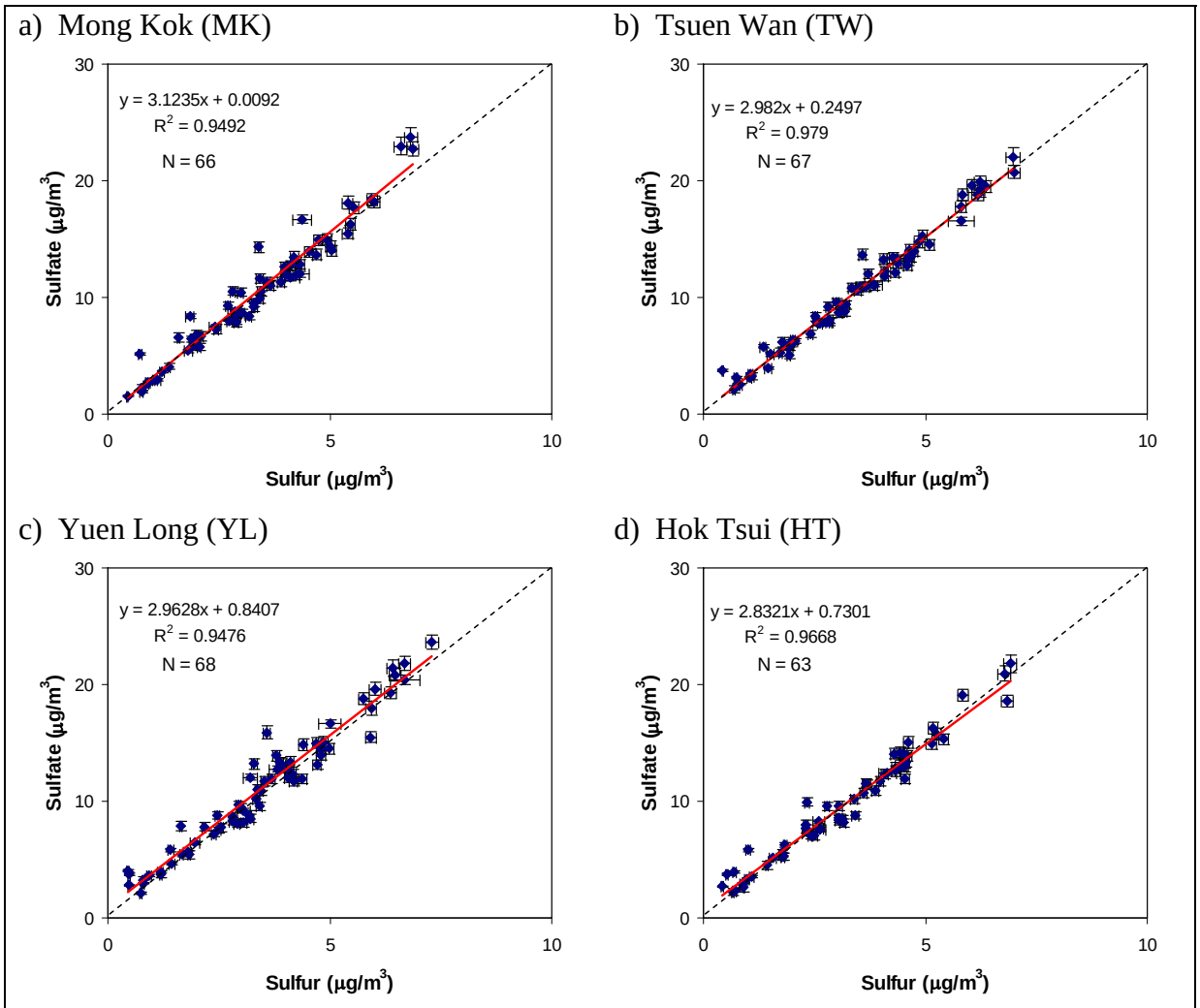

Statistics\Site	MK	TW	YL	HT	All
Slope	3.123 ± 0.009	2.982 ± 0.054	2.963 ± 0.086	2.832 ± 0.067	2.978 ± 0.039
Intercept	0.009 ± 0.334	0.250 ± 0.207	0.841 ± 0.330	0.730 ± 0.241	0.444 ± 0.145
R^2	0.949	0.979	0.948	0.967	0.958
N	66	67	68	63	264
Avg(X)	3.326	3.429	3.453	3.178	3.350
Avg(Y)	10.398	10.475	11.071	9.732	10.432
Avg(Y/X)	3.167 ± 0.617	3.155 ± 0.727	3.422 ± 0.998	3.260 ± 0.817	3.252 ± 0.806

Figure 3-3. Scatter plots of sulfate versus sulfur measurements from $PM_{2.5}$ data acquired at: a) the MK site; b) the TW site; c) the YL site; and d) the HT site.

3.4.2.2 Chloride versus Chlorine

Chloride (Cl^-) was measured by IC on quartz-fiber filters, and chlorine (Cl) was measured by XRF on Teflon-membrane filters. Because chloride is the water-soluble portion of chlorine, the chloride-to-chlorine ratio is expected to be less than unity. Figure 3-4 shows that moderate correlations (R^2 = 0.78) were found between $PM_{2.5}$ chloride and chlorine measurements, with a slope larger than unity (1.46–1.81) and substantial intercepts (0.04–0.17 µg/m^3) among all the sites. The uncertainties of chloride measurements were higher at

low concentrations because chloride's elution peak in ion chromatographic analysis is close to the distilled water dip which, in turn, shifts the baseline of the chromatogram (Chow and Watson, 1999). In addition, chlorine collected on the Teflon filter may be lost through volatilization because XRF analysis is conducted in a vacuum chamber. Such losses are especially apparent when chlorine concentrations are low.

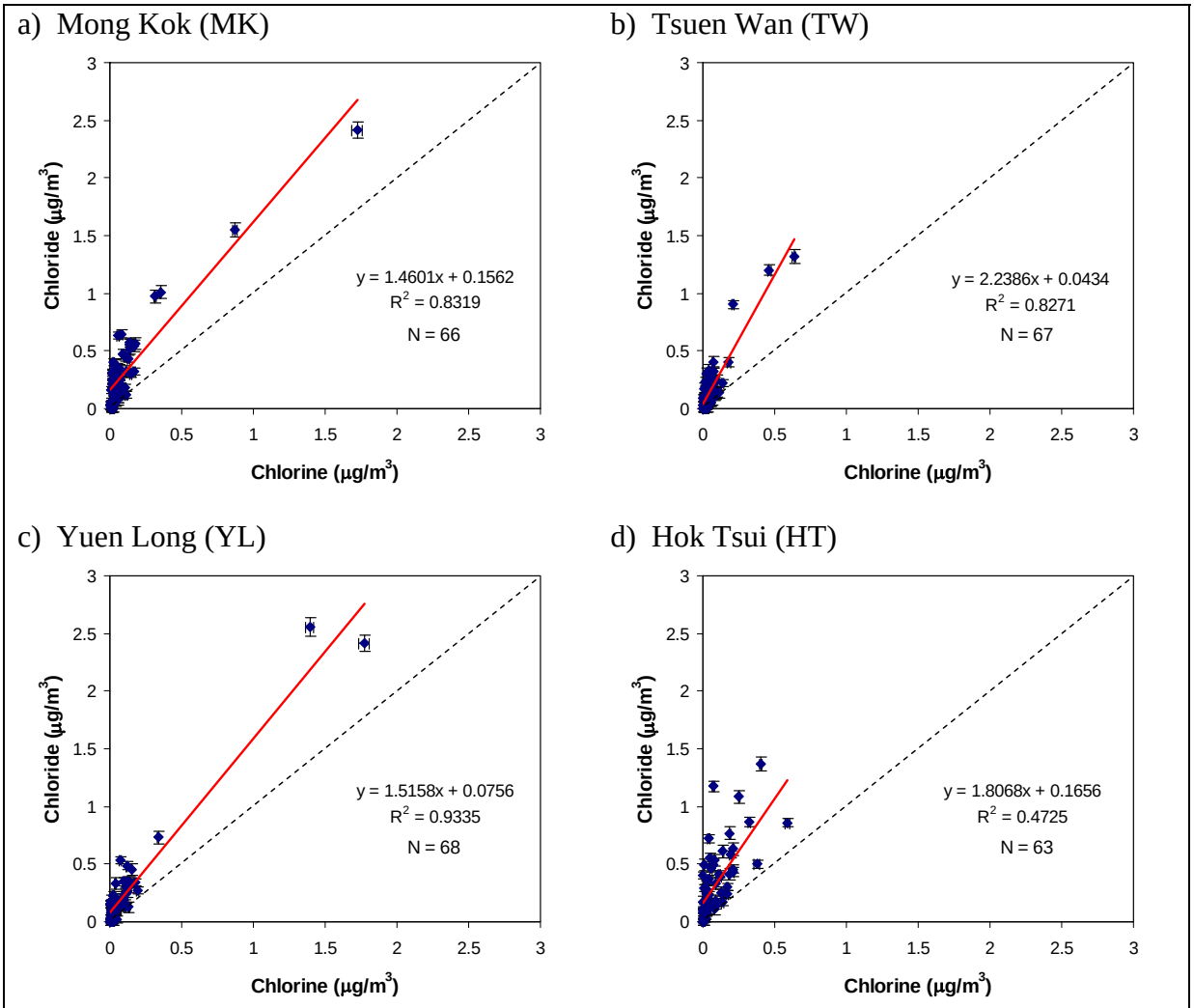

Statistics\Site	MK	TW	YL	HT	All
Slope	1.460 ± 0.082	2.239 ± 0.127	1.516 ± 0.050	1.807 ± 0.244	1.571 ± 0.051
Intercept	0.156 ± 0.021	0.043 ± 0.014	0.076 ± 0.014	0.166 ± 0.035	0.120 ± 0.011
R^2	0.832	0.827	0.934	0.473	0.781
N	66	67	68	63	264
Avg(X)	0.102	0.058	0.100	0.088	0.087
Avg(Y)	0.305	0.173	0.226	0.324	0.256
Avg(Y/X) *	5.586 ± 4.465	4.909 ± 3.550	4.134 ± 3.663	7.160 ± 12.178	5.472 ± 6.986

* Data with concentration less than twice the analytical uncertainty are excluded.

Figure 3-4. Scatter plots of chloride versus chlorine measurements from $PM_{2.5}$ data acquired at: a) the MK site; b) the TW site; c) the YL site; and d) the HT site.

3.4.2.3 Soluble Potassium versus Total Potassium

Figure 3-5 displays the scatter plots of soluble potassium versus total potassium concentrations. Soluble potassium (K^+) was acquired by atomic absorption spectrophotometry (AAS) analysis on quartz-fiber filters, and total potassium (K) was

a) Mong Kok (MK)

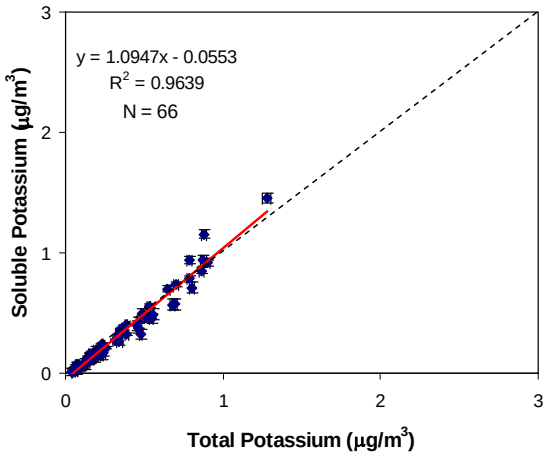

b) Tsuen Wan (TW)

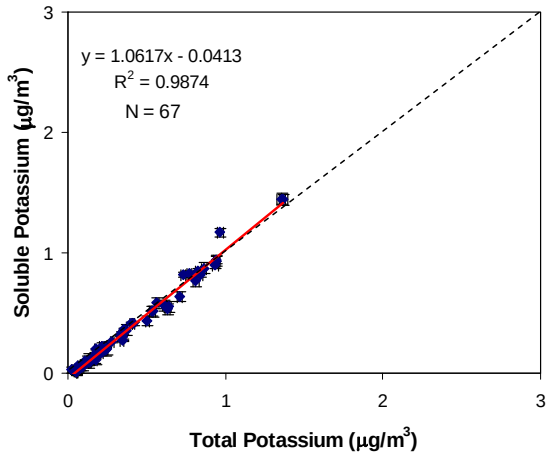

c) Yuen Long (YL)

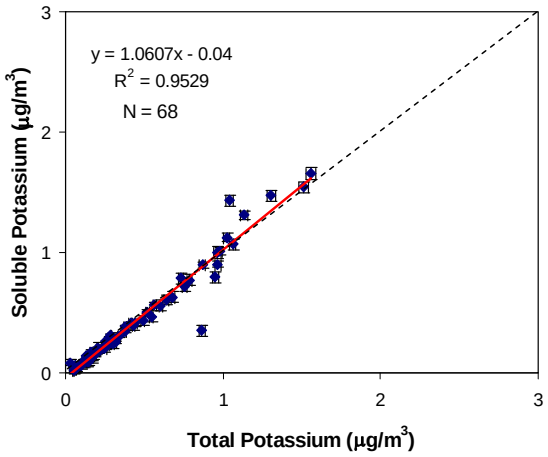

d) Hok Tsui (HT)

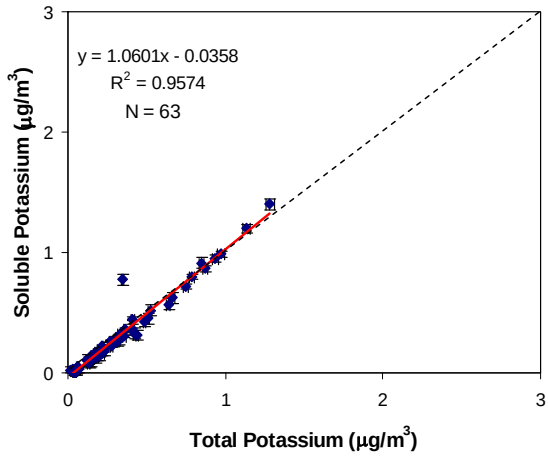

Statistics\Site	MK	TW	YL	HT	All
Slope	1.095 ± 0.026	1.062 ± 0.015	1.061 ± 0.029	1.060 ± 0.029	1.067 ± 0.013
Intercept	-0.055 ± 0.012	-0.041 ± 0.007	-0.040 ± 0.017	-0.036 ± 0.012	-0.042 ± 0.006
R^2	0.964	0.987	0.953	0.957	0.965
N	66	67	68	63	264
Avg(X)	0.344	0.368	0.435	0.317	0.367
Avg(Y)	0.321	0.349	0.421	0.300	0.349
Avg(Y/X) *	0.884 ± 0.148	0.898 ± 0.126	0.952 ± 0.313	0.898 ± 0.223	0.909 ± 0.217

* Data with concentration less than twice the analytical uncertainty are excluded.

Figure 3-5. Scatter plots of soluble potassium versus total potassium measurements from $PM_{2.5}$ data acquired at: a) the MK site; b) the TW site; c) the YL site; and d) the HT site.

acquired by XRF analysis on Teflon-membrane filters. Since potassium concentrations are often used as an indicator of vegetative burning, it is important to assure the validity of the K^+ measurement.

This analysis shows that K^+ concentrations are low to moderate throughout the study area and period, even though an average of ~90% of the total potassium is in its soluble state. The average y/x ratio of K^+/K was 0.91 ± 0.22. The high K^+/K ratios imply that vegetative burning or long-range transport of wildfire emissions are prominent source of potassium in the study area.

3.4.2.4 Ammonium Balance

Ammonium nitrate (NH_4NO_3), ammonium sulfate ($[NH_4]_2SO_4$), and ammonium bisulfate (NH_4HSO_4), are the most likely nitrate and sulfate compounds to be found in Hong Kong. Some sodium nitrate ($NaNO_3$) and/or sodium sulfate (Na_2SO_4) may also be present at the coastal sites, which may be attributable to transport by prevailing winds from the Pacific Ocean into Hong Kong, especially during summer. Ammonium (NH_4^+) can be calculated based on the stoichiometric ratios of the different compounds and compared with that was measured. In Figure 3-6, ammonium is calculated from nitrate and sulfate, assuming that all nitrate was in the form of ammonium nitrate and all sulfate was in the form of either ammonium sulfate (i.e., calculated ammonium = [0.38 × sulfate] + [0.29 × nitrate]) or ammonium bisulfate (i.e., ammonium = [0.192 × sulfate] + [0.29 × nitrate]). These calculated values were compared with the measured values for ammonium.

If a significant amount of sodium sulfate is present due to contamination, the calculated ammonium would greatly exceed measured values. As shown in Figure 3-6, the ratio of calculated and measured ammonium is 2.04 ± 2.50 assuming ammonium sulfate and 1.15 ± 1.35 assuming ammonium bisulfate (both greater than unity). At HT, average measured ammonium agrees with calculated ammonium assuming ammonium bisulfate within 15% (2.682 μg m^{-3} versus 2.328 μg m^{-3}). This situation is rarely observed where ammonium bisulfate accounts for a majority of sulfate. The chromatograms from ion chromatography analysis for nitrate and sulfate and graphs from automated colorimetry analysis for ammonium were examined, but no anomalies were found. It had been explained by the presence of coarse-particle sulfate and/or nitrate salts that might be associated with water-soluble Na^+, K^+, or Ca^{++} ions. Since this occurs for $PM_{2.5}$ instead of PM_{10}, however, Na^+, K^+, or Ca^{++} ions likely resulted from contamination rather than coarse particles.

In any cases, calculated ammonium is still highly correlated with measured ammonium (R^2 > 0.93). The slopes seen in these figures average 1.11 ± 0.06 assuming ammonium sulfate, and 0.68 ± 0.01 assuming ammonium bisulfate, close to slopes found in earlier years. This implies that a majority of the sulfate was neutralized in the form of ammonium sulfate during the study period. The intercepts, however, are much higher than before, averaging 18–21% of calculated ammonium. These data thus imply that the sulfate contamination, if any, varied less than ambient sulfate concentration across all measured samples, and likely have a level between 1.0 and 1.5 μg/m^3.

a) Mong Kok (MK)

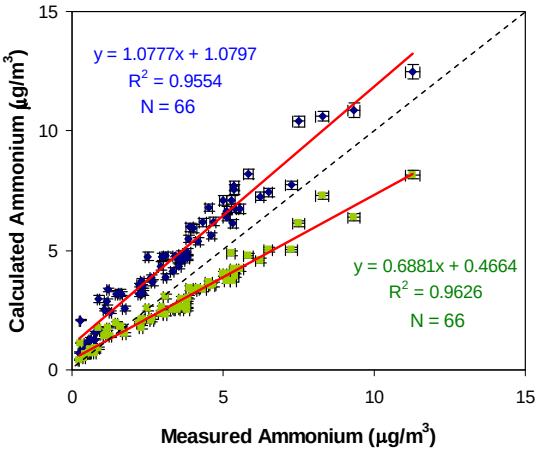

b) Tsuen Wan (TW)

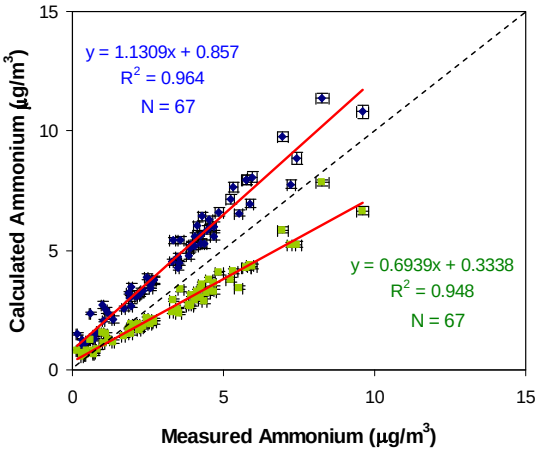

c) Yuen Long (YL)

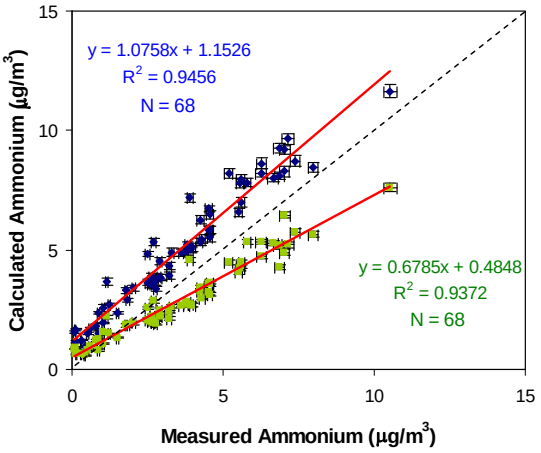

d) Hok Tsui (HT)

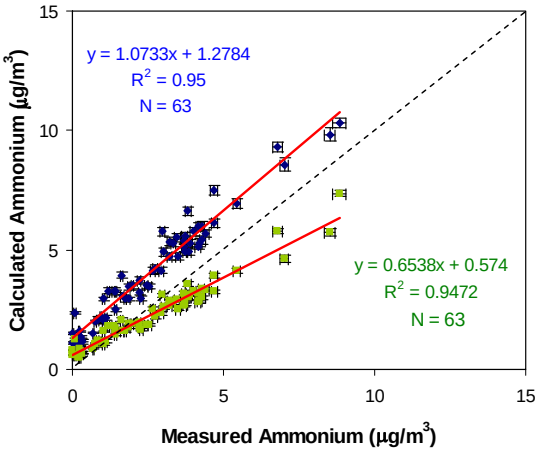

Statistics\Site	MK	TW	YL	HT	All
Ammonium Sulfate (blue dots)					
Slope	1.078 ± 0.029	1.131 ± 0.027	1.076 ± 0.032	1.073 ± 0.032	1.084 ± 0.015
Intercept	1.080 ± 0.120	0.857 ± 0.106	1.153 ± 0.134	1.278 ± 0.105	1.109 ± 0.058
R^2	0.955	0.964	0.946	0.950	0.953
N	66	67	68	63	264
Avg(X)	3.444	3.309	3.558	2.682	3.257
Avg(Y)	4.791	4.600	4.980	4.157	4.640
Avg(Y/X) *	1.700 ± 0.909	1.739 ± 1.212	2.188 ± 3.012	2.558 ± 3.753	2.036 ± 2.503
Ammonium Bisulfate (green dots)					
Slope	0.688 ± 0.017	0.694 ± 0.020	0.678 ± 0.022	0.654 ± 0.020	0.679 ± 0.010
Intercept	0.466 ± 0.070	0.334 ± 0.079	0.485 ± 0.091	0.574 ± 0.066	0.467 ± 0.038
R^2	0.963	0.948	0.937	0.947	0.949
N	66	67	68	63	264
Avg(X)	3.444	3.309	3.558	2.682	3.257
Avg(Y)	2.836	2.630	2.899	2.328	2.679
Avg(Y/X) *	0.984 ± 0.485	0.978 ± 0.656	1.237 ± 1.644	1.403 ± 2.010	1.146 ± 1.349

* Data with concentration less than twice the analytical uncertainty are excluded.

Figure 3-6. Scatter plots of calculated ammonium versus measured ammonium from $PM_{2.5}$ data acquired at: a) the MK site; b) the TW site; c) the YL site; and d) the HT site.

3.4.3 Anion and Cation Balance

The anion (NO_3^-, $SO_4^=$, Cl^-) and cation (NH_4^+, Na^+, K^+) balance in Figure 3-7 also shows a deficiency in cations that is not accounted for by measured anions. The correlations are high ($R^2 > 0.94$) in the $PM_{2.5}$ size fraction. The difference may be attributable to unmeasured H^+. The difference could also be due to the presence of coarse-particle sulfate

a) Mong Kok (MK)

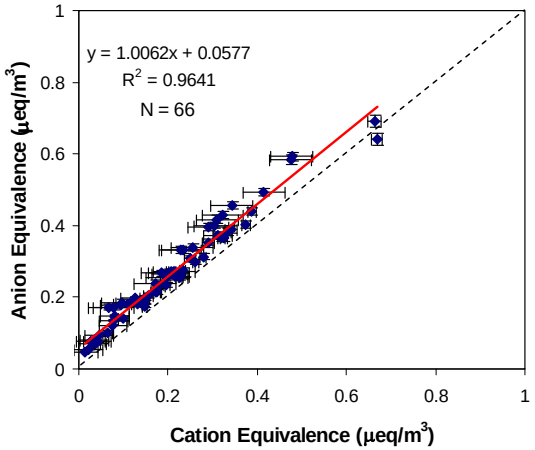

b) Tsuen Wan (TW)

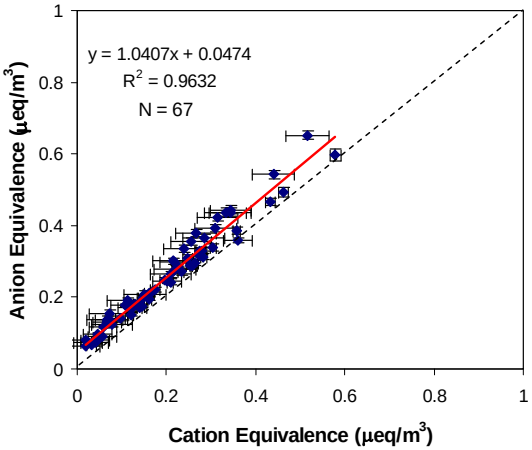

c) Yuen Long (YL)

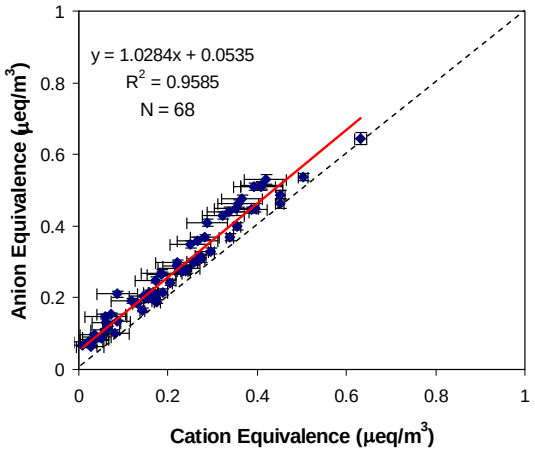

d) Hok Tsui (HT)

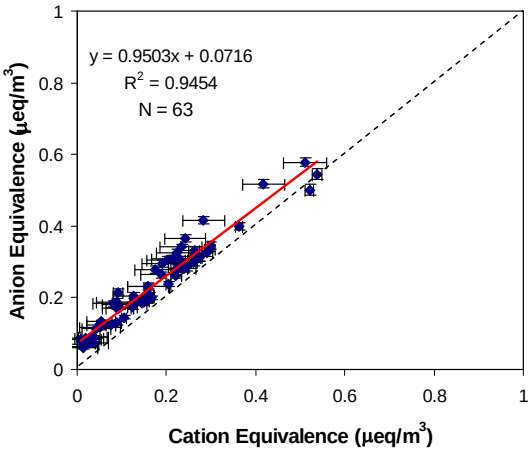

Statistics\Site	MK	TW	YL	HT	All
Slope	1.006 ± 0.024	1.041 ± 0.025	1.028 ± 0.026	0.950 ± 0.029	1.007 ± 0.013
Intercept	0.058 ± 0.006	-0.047 ± 0.006	0.053 ± 0.007	0.072 ± 0.006	0.058 ± 0.003
R^2	0.964	0.963	0.958	0.945	0.958
N	66	67	68	63	264
Avg(X)	0.213	0.202	0.220	0.174	0.203
Avg(Y)	0.272	0.258	0.280	0.237	0.262
Avg(Y/X) *	1.330 ± 0.217	1.313 ± 0.221	1.286 ± 0.191	1.392 ± 0.319	1.328 ± 0.239

* Data with concentration less than twice the analytical uncertainty are excluded.

Figure 3-7. Scatter plots of cation versus anion measurements from $PM_{2.5}$ data acquired at: a) the MK site; b) the TW site; c) the YL site; and d) the HT site.

and/or nitrate in forms other than ammonium, sodium, or potassium salts. However, Figure 3-7 generally shows a good balance between anions and cations with a regression slope of ~1.

3.4.4 IMPROVE_A TOR versus TOT Protocol for Carbon Measurements

EC and OC determined by IMPROVE_A TOR and TOT methods for samples from each site and all sites combined are compared in Figure 3-8. TOT EC can be significantly lower than TOR EC because char imbedded within filter can absorb light more efficiently than char and/or EC on the filter surface (Chow et al., 2004; Chen et al., 2004; Subraminan et al., 2006). TOT is more influenced by the within-filter char than TOR. On the other hand, TOR OC is typically lower than TOT OC as OC complements EC in the samples. At all sites the correlation between TOR and TOT EC exceeds R^2 = 0.96. OC also exhibits good correlation with R^2 = 0.98.

At the MK site, ambient concentrations of EC and OC were much higher than the other sites, and results from the TOR and TOT protocols are less correlated (EC: R^2 = 0.69; OC: R^2 = 0.93). The laser split becomes uncertain as the filter loading becomes too high (i.e., reflectance signals are saturated while transmittance signals are not detected). On the contrary, correlations between EC (R^2 = 0.93) and OC (R^2 = 0.99) measurements are much better at the background HT site. Overall, the adoption of different analytical protocols can yield significantly different OC and EC measurements, and this will influence the OC/EC partitioning and mass closure in $PM_{2.5}$.

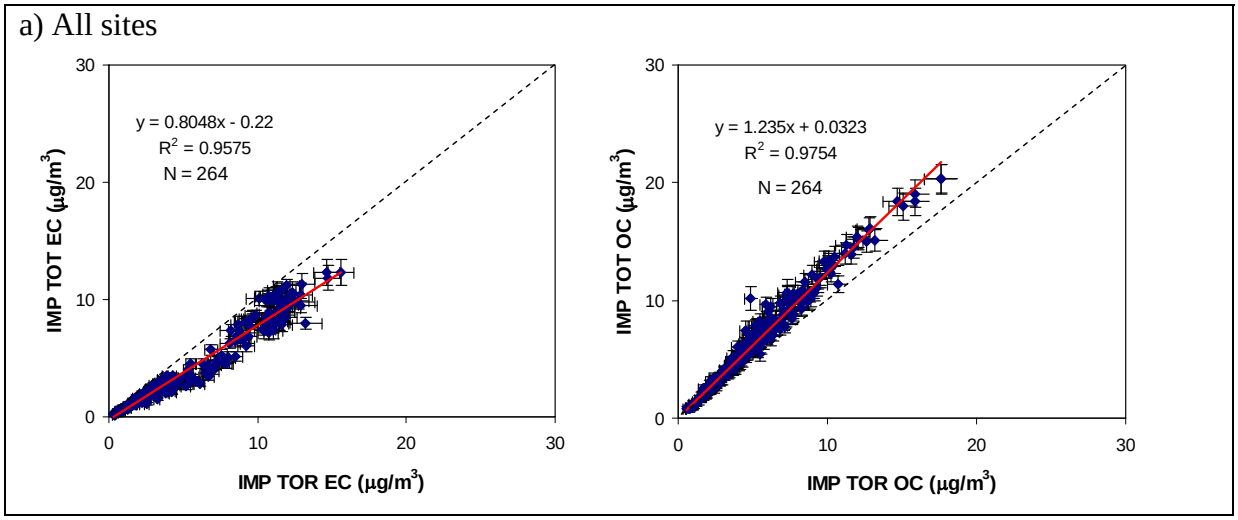

Figure 3-8. Comparisons of EC and OC determined by IMPROVE_A TOR and TOT methods as defined in Section 2.2 at: a) all four sites, b) the MK site, c) the TW site, d) the YL site, and e) the HT site.

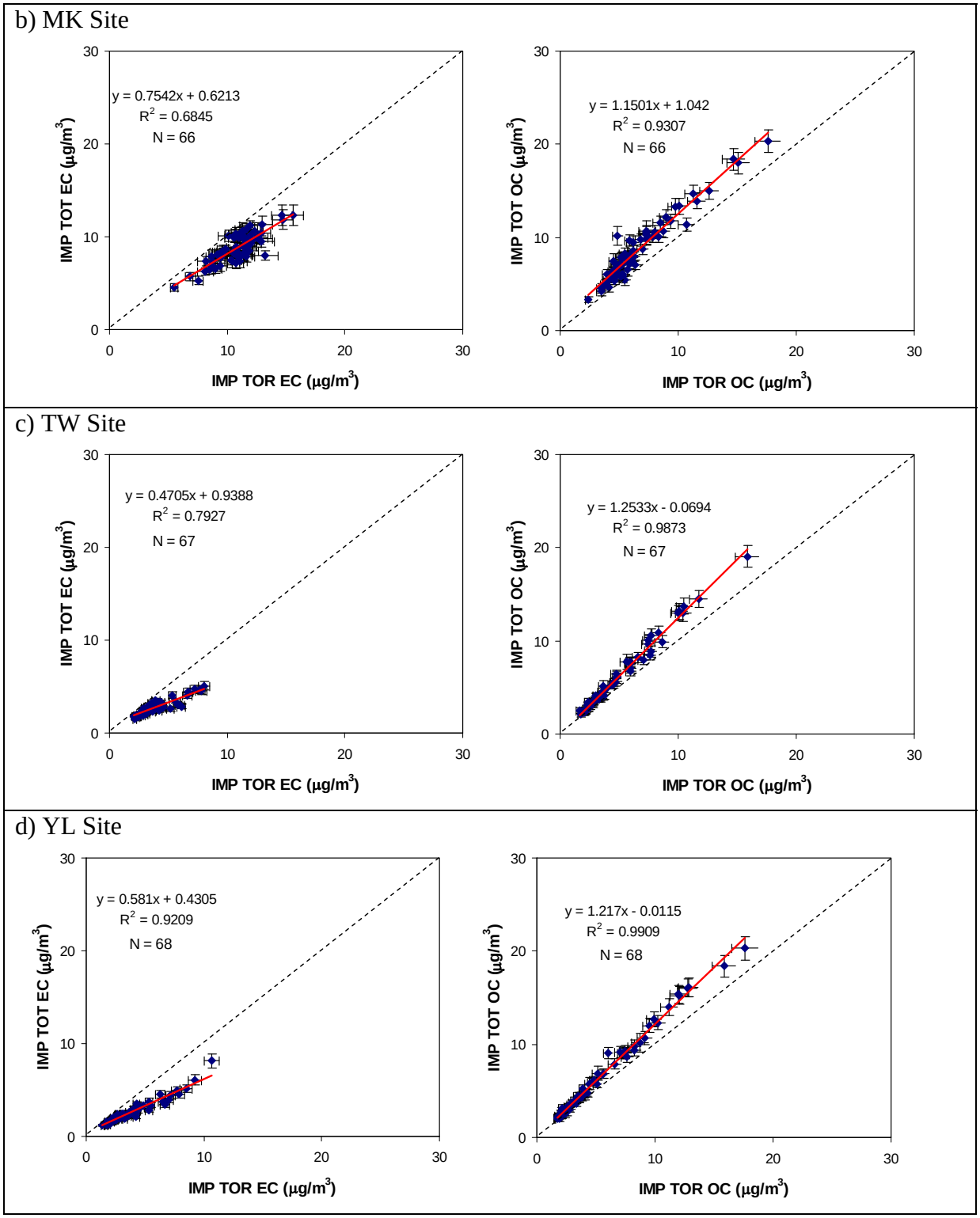

Figure 3-8. Continued.

e) HT Site

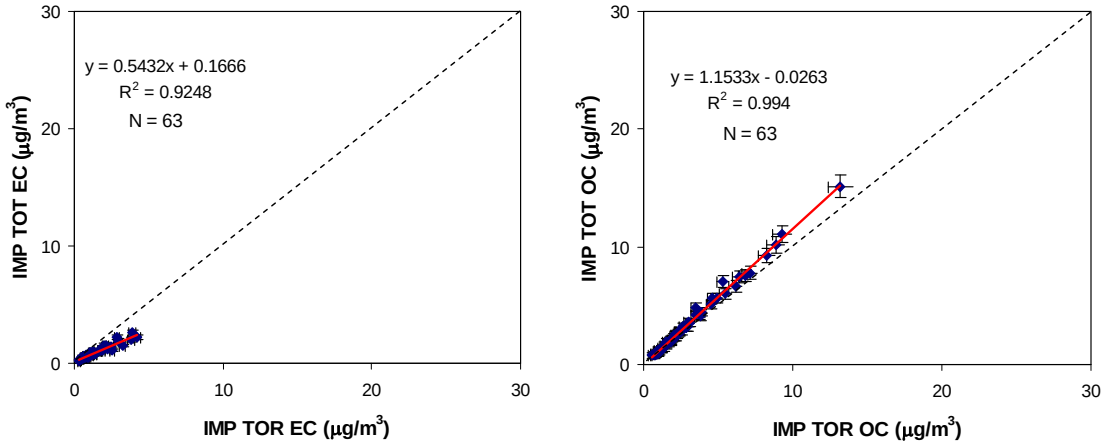

Statistics\Site	MK	TW	YL	HT	All
TOT EC vs TOR EC					
Slope	0.754 ± 0.064	0.470 ± 0.030	0.581 ± 0.021	0.543 ± 0.020	0.805 ± 0.010
Intercept	0.621 ± 0.702	0.939 ± 0.123	0.430 ± 0.089	0.167 ± 0.032	-0.220 ± 0.066
R^2	0.685	0.793	0.921	0.925	0.958
N	66	67	68	63	264
Avg(X)	10.824	3.884	3.737	1.316	4.968
Avg(Y)	8.784	2.766	2.601	0.881	3.778
Avg(Y/X)	0.813 ± 0.084	0.738 ± 0.110	0.729 ± 0.104	0.720 ± 0.117	0.750 ± 0.110
TOT OC vs TOR OC					
Slope	1.150 ± 0.039	1.253 ± 0.018	1.217 ± 0.014	1.153 ± 0.011	1.235 ± 0.012
Intercept	1.042 ± 0.283	-0.069 ± 0.097	-0.012 ± 0.092	-0.026 ± 0.044	0.032 ± 0.071
R^2	0.931	0.987	0.991	0.994	0.975
N	66	67	68	63	264
Avg(X)	6.618	4.672	5.266	2.980	4.908
Avg(Y)	8.654	5.786	6.397	3.410	6.093
Avg(Y/X)	1.326 ± 0.166	1.233 ± 0.089	1.209 ± 0.085	1.135 ± 0.075	1.227 ± 0.128

Figure 3-8. Continued.

3.4.5 Reconstructed versus Measured Mass

Major PM components can be used to reconstruct $PM_{2.5}$ mass. The major components should include: 1) geological material (estimated as 1.89×Al + 2.14×Si + 1.4×Ca + 1.43×Fe to account for unmeasured oxides), 2) organic matter (OM: 1.4×OC to account for unmeasured hydrogen and oxygen), 3) soot (elemental carbon), 4) ammonium sulfate, 5) ammonium nitrate, and 6) noncrustal trace elements (sum of other-than-geological trace elements). The difference between the constructed mass and the measured mass is referred to as unidentified mass. Considering the potential contamination of filter blanks by sodium sulfate and potassium sulfate, it is decided that sulfate, nitrate, ammonium, soluble sodium, and total potassium are counted separately in the reconstructed mass, thus:

[Reconstructed $PM_{2.5}$ mass] = [geological material] + [organic matter] + [soot] + [sulfate] + [ammonium] + [nitrate] + [soluble sodium] + [total potassium] + [(noncrustal, Na^+, and K) trace elements]

The reconstructed mass are highly correlated to the measured mass at R^2 = 0.98 for

all-site data (Figure 3-9). In contrast to the sum-of-species-versus-mass comparison in Figure 3-2, unaccounted mass is largely eliminated when unmeasured oxygen and hydrogen were factored in. This confirms the validity of gravimetric and chemical measurements, though the regression intercept still accounts for 1 – 12% of reconstructed mass.

a) Mong Kok (MK)

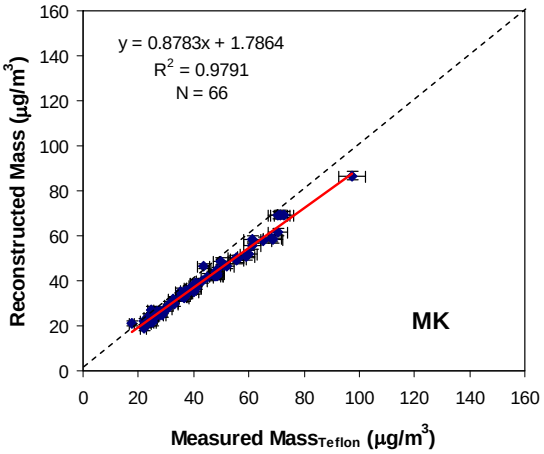

b) Tsuen Wan (TW)

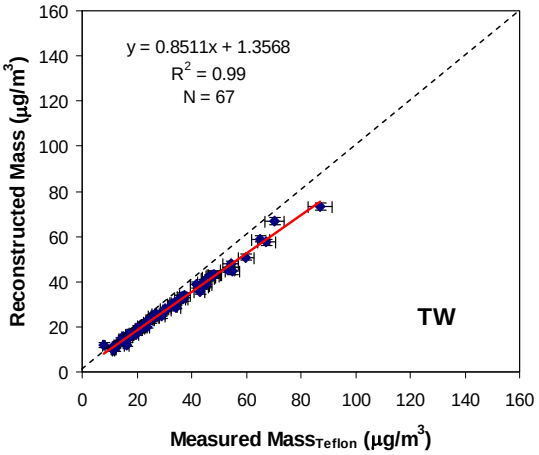

c) Yuen Long (YL)

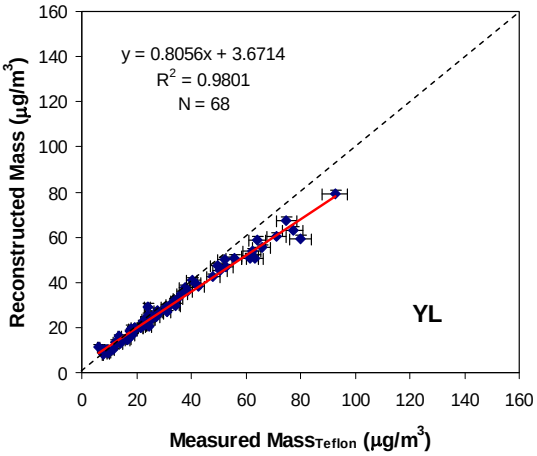

d) Hok Tsui (HT)

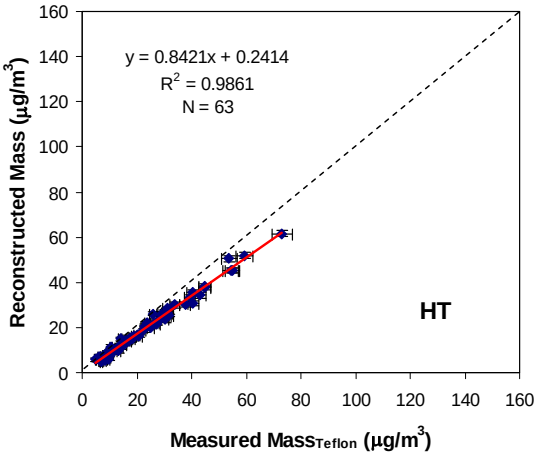

Statistics\Site	MK	TW	YL	HT	All
Slope	0.878 ± 0.016	0.851 ± 0.011	0.806 ± 0.014	0.842 ± 0.013	0.860 ± 0.008
Intercept	1.786 ± 0.729	1.357 ± 0.377	3.671 ± 0.551	0.241 ± 0.373	1.353 ± 0.284
R^2	0.979	0.990	0.980	0.986	0.980
N	66	67	68	63	264
Avg(X)	42.596	31.567	33.406	25.128	33.261
Avg(Y)	39.198	28.222	30.585	21.402	29.947
Avg(Y/X)	0.927 ± 0.59	0.909 ± 0.088	0.960 ± 0.147	0.861 ± 0.096	0.915 ± 0.108

Figure 3-9. Scatter plots of reconstructed mass versus measured $PM_{2.5}$ mass from Teflon filters at: a) the MK site; b) the TW site; c) the YL site; and d) the HT site. Uncertainties of the measured mass are assumed to be 5% of concentration.

Figure 3-10 shows the annual average composition (%) of these major components to $PM_{2.5}$ mass. The unidentified mass was set to zero when the reconstructed mass is greater than the measured mass (i.e. unidentified mass is negative), and the mass fractions of the major components were adjusted accordingly. This never occurred this year. At MK, TW, YL, and HT, the unidentified mass was ~8%, 11%, 8%, and 15% of measured mass, respectively. To measure the gravimetric mass, Teflon filters were weighted at 30–40% relative humidity. There could, however, still be residual water with ammonium sulfate and ammonium nitrate that accounted for the unidentified mass. Overall, the reconstructed mass agrees with the measured mass within ~15%.

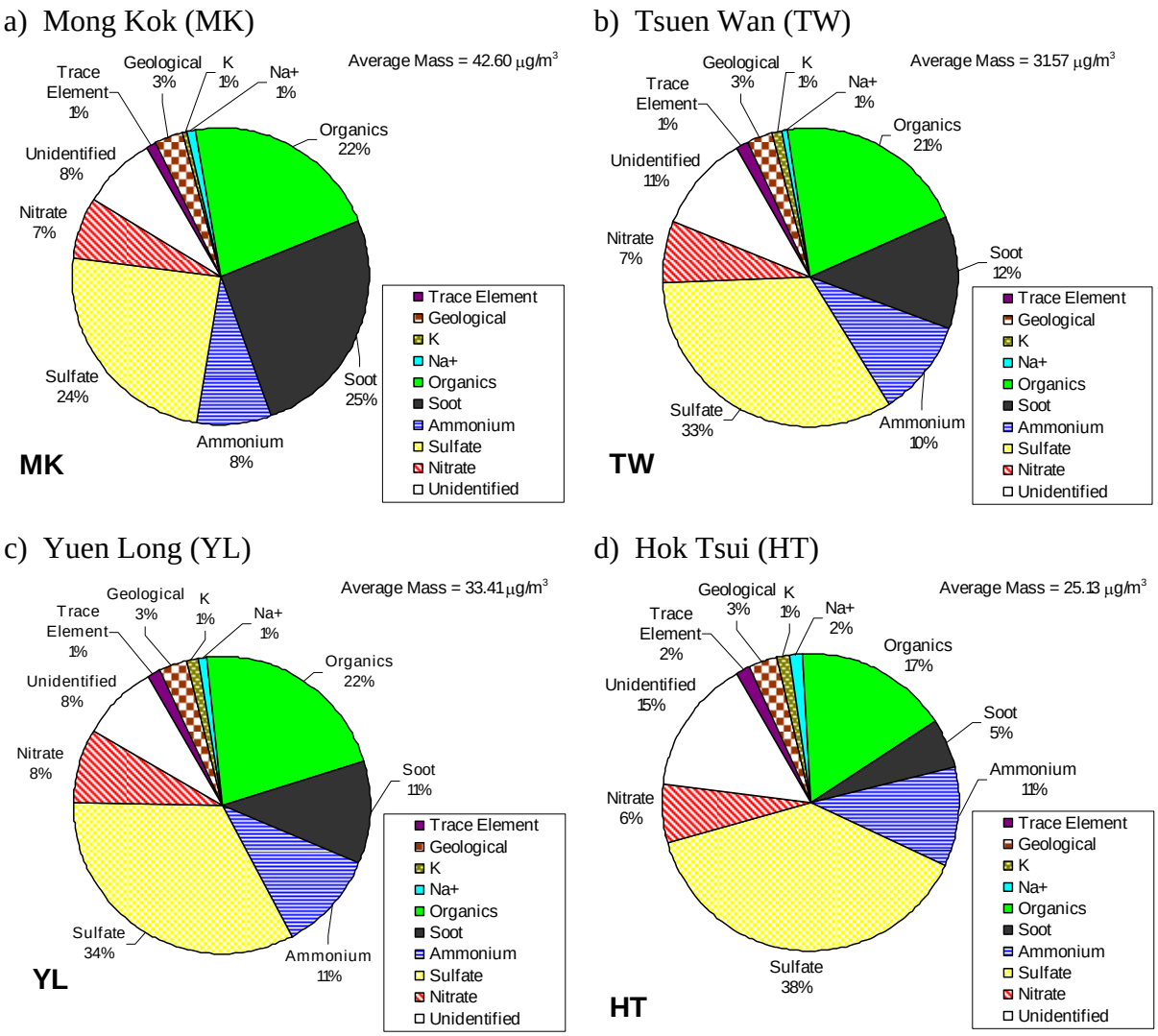

Figure 3-10. Material balance charts for $PM_{2.5}$ data acquired at: a) the MK site; b) the TW site; c) the YL site; and d) the HT site. The major components of reconstructed mass include: 1) geological material, 2) total potassium, 3) soluble sodium, 4) organic matter, 5) soot (elemental carbon), 6) ammonium, 7) sulfate, 8) nitrate, 9) noncrustal, non-K, and non-Na^+ trace elements listed in Table 3-4, and 7) unidentified mass (difference between measured mass and the sum of the major components).

Figure 3-11 demonstrates the average reconstructed mass for the highest and lowest 20% $PM_{2.5}$ days at the four sites. On high $PM_{2.5}$ days, the increased mass consists mostly of ammoniated sulfate and OM, both of which can be of secondary origin. High sulfate and OM concentrations usually occurred simultaneously across all four sites, suggesting the presence of variable regional sources. The change in EC concentration, a primary combustion tracer, is relatively limited at MK. Nearby traffic emissions provide a consistent source for EC at the urban site(s). The HT site does not have significant sources nearby, so most of the pollutants measured at this site were probably transported from distant urban areas. The unidentified mass are much more significant for high $PM_{2.5}$ days, probably also due to increased ammonium sulfate, and associated water, concentrations.

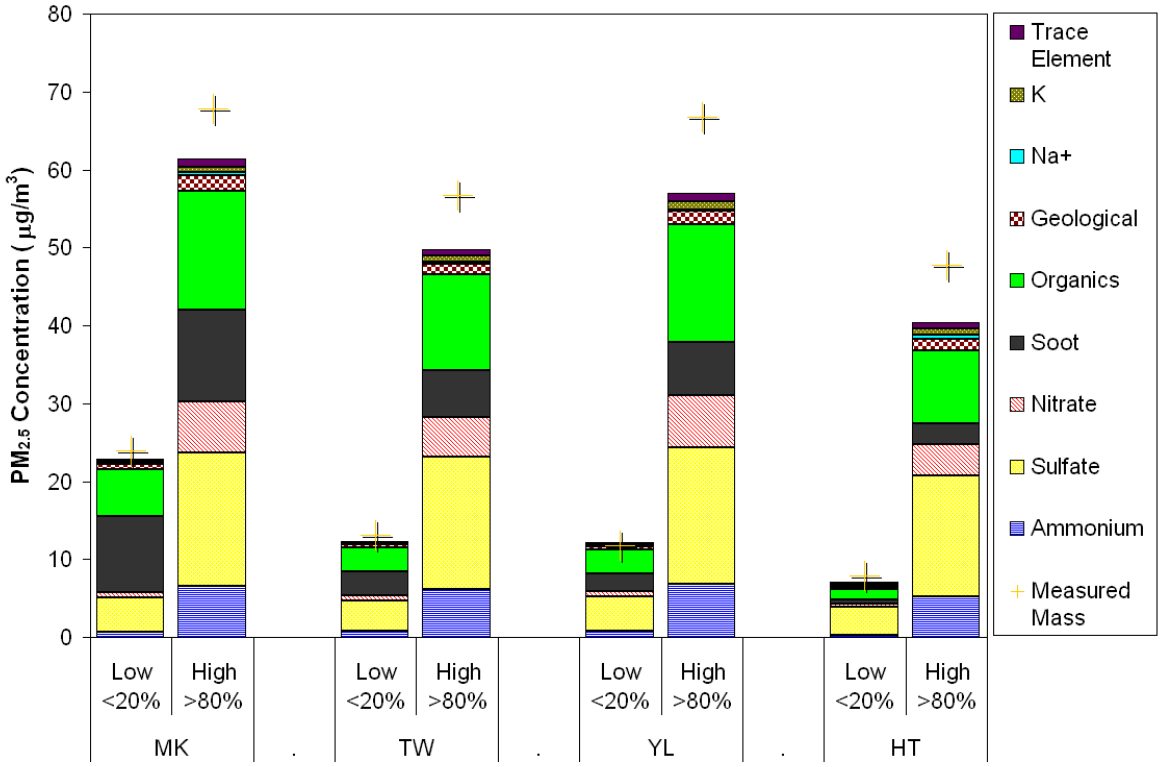

Figure 3-11. Mean reconstructed mass and chemical composition for the highest and lowest 20% $PM_{2.5}$ days at the Mong Kok (MK), Tsuen Wan (TW), Yuen Long (YL), and Hok Tsui (HT) sites.

4 COMPARISON TO THE FIRST AND SECOND YEAR STUDY

Table 4-1 shows the side-by-side comparison of the three year study of samples collected during 2000–2001, 2004–2005, and current 2009 periods (note: to compare on annual basis, only 12-month data in 2009 were used). An additional site (Yuen Long [YL]) was added during the second year, so no comparisons can be made for the first year. $PM_{2.5}$ mass concentrations show decreasing trends through all comparisons except for HT during the 2001–2009 time frame, where $PM_{2.5}$ increased slightly by 1.9%. MK and TW sites exhibited a decrease of 28.6% and 10.3% during the same period. Between 2005 and 2009, $PM_{2.5}$ decreased by 15.2 – 23.1% across the four sites.

Nitrate, sulfate and ammonium concentrations trended upward from the first year study to the second year study and downward from the second year to the third year study. In eight years (2001–2009), sulfate and nitrate increased by 11.8% and 113.1%, respectively, at the HT sites and by 9.6% and 70.0%, respectively, at the MK site. The increase of sulfate is partially attributed to "residual sulfate" on QMA quartz-fiber filters, as the increase in elemental sulfur measured on Teflon filters is substantially less (3.7% and -4.1%). Ammonium increased consistently across the MK, TW, and HT sites (7.2–22.0%), and much of the additional ammonium could be associated with nitrate. Sulfate and ammonium reached maximums in 2005, and have decreased 18.9–20.6% and 14.0–24.8%, respectively since then. Sulfur concentration also decreased by 22.2 – 25.2%. Secondary ammonium sulfate is often attributed to regional resources (Louie et al., 2005b). Their decrease over the territory indicates the improvement in the regional air quality. Nitrate concentration, on the other hand, has been increasing at MK, TW, and HT (2005–2009), likely due to the nitrate substitution effect as the sulfate concentration dropped (Davidson et al., 2005).

Organic and elemental carbon both showed a significant decrease in concentration since 2001 (-62.4% and -47.5% [2001–2009] respectively) at the MK site. The reduction in carbon levels at the roadside site suggests the significant contributions from the programs about reduction in vehicular emissions, tightening diesel fuel and vehicle emission standards, over these years. Whereas the other three sites, TW, YL, and HT also experienced decreasing OC and EC concentrations. From 2005 to 2009, OC was reduced by 31.2 – 36.9% and EC was decreased by 39.9 – 47.0% across the three sites.

Crustal elements (Al, Si, Ca, and Fe) generally trended downward in the 2001–2009 and 2005–2009 period. The concentrations of soluble sodium and potassium also decreased substantially across all four sites, but such trends were not observed for chloride. This may result from over-subtraction of blank levels for Na^+ and K^+ in the current study but warrants further investigations to determine the degree of environmental cause (e.g., suppression of wildfires and agricultural burning) to the reductions. Several other elemental concentrations show what appear to be significant changes (e.g., a nearly 90% decrease in measured phosphorous concentrations between 2005–2009). However, the increase or decrease in micrograms per cubic meter concentrations is actually quite small. It should also be noted that the first year study filters were analyzed on an older model Kevex energy dispersive XRF machine which was replaced with a new system prior to the analysis of the second year and current study filter samples. The new system is a PanAlytical Epsilon 5 energy dispersive XRF system. While both systems operate under the same basic analysis principles, both the hardware and software have been upgraded with the new system.

Table 4-1. Side-by-side comparison of the three year study of samples (in μg/m^3) collected during 2000–2001, 2004–2005, and current 2009 (1/5/2009 – 12/29/2009) period. Carbon concentrations are from the IMPROVE_A TOR protocol.

	2001 MK	2001 TW	2001 HT	2005 MK	2005 TW	2005 YL	2005 HT	2009 MK	2009 TW	2009 YL	2009 HT	2001-2009 % Chg. (MK)	2001-2009 % Chg. (TW)	2001-2009 % Chg. (HT)	2005-2009 % Chg. (MK)	2005-2009 % Chg. (TW)	2005-2009 % Chg. (YL)	2005-2009 % Chg. (HT)
Teflon Mass	58.2806	34.1221	23.6575	53.0228	38.5926	41.3102	28.4374	41.6004	30.6115	31.7805	24.1048	-28.6	-10.3	1.9	-21.5	-20.7	-23.1	-15.2
Quartz Mass	62.5022	37.2802	25.8475	54.8681	40.7482	43.9080	29.6432	45.9239	34.0026	36.3433	25.9449	-26.5	-8.8	0.4	-16.3	-16.6	-17.2	-12.5
Cl-	0.2555	0.1376	0.1428	0.2827	0.1257	0.2642	0.1241	0.3121	0.1746	0.2130	0.2975	22.2	27.0	108.4	10.4	38.9	-19.4	139.8
NO3-	1.6527	1.3426	0.7079	2.4040	1.6350	2.8642	0.7619	2.8089	2.0305	2.4194	1.5082	70.0	51.2	113.1	16.8	24.2	-15.5	97.9
SO4=	9.5022	9.1721	8.6410	12.8397	13.1737	13.9100	11.9062	10.4139	10.4805	11.0410	9.6566	9.6	14.3	11.8	-18.9	-20.4	-20.6	-18.9
NH4+	3.1739	2.9645	2.1570	4.4003	4.0702	4.6173	3.0590	3.4024	3.2684	3.4701	2.6313	7.2	10.3	22.0	-22.7	-19.7	-24.8	-14.0
Na+	0.3978	0.3972	0.6794	0.4228	0.3624	0.3745	0.5265	0.3204	0.2112	0.2624	0.3804	-19.5	-46.8	-44.0	-24.2	-41.7	-29.9	-27.7
K+	0.4567	0.4921	0.4026	0.4787	0.4862	0.5615	0.4333	0.2784	0.3077	0.3649	0.2594	-39.0	-37.5	-35.6	-41.8	-36.7	-35.0	-40.1
OC	16.6419	8.6898	4.2256	11.1770	6.9317	7.2348	3.9213	6.2623	4.3756	4.8341	2.6972	-62.4	-49.6	-36.2	-44.0	-36.9	-33.2	-31.2
EC	20.2884	5.3705	1.6824	14.1154	6.2578	6.1939	2.2770	10.6608	3.7598	3.4875	1.2058	-47.5	-30.0	-28.3	-24.5	-39.9	-43.7	-47.0
TC	36.9105	14.0405	5.8897	25.2839	13.1811	13.4203	6.1899	16.9116	8.1239	8.3101	3.8915	-54.2	-42.1	-33.9	-33.1	-38.4	-38.1	-37.1
Al	0.1139	0.1146	0.1091	0.1408	0.1414	0.1448	0.1223	0.0986	0.0828	0.0913	0.0828	-13.4	-27.8	-24.1	-30.0	-41.5	-36.9	-32.4
Si	0.4778	0.3870	0.3489	0.3469	0.3141	0.3221	0.2546	0.2485	0.1853	0.2073	0.1685	-48.0	-52.1	-51.7	-28.3	-41.0	-35.6	-33.8
P	0.0092	0.0050	0.0028	0.1886	0.1950	0.1917	0.1747	0.0225	0.0237	0.0229	0.0225	145.3	374.1	699.2	-88.1	-87.8	-88.0	-87.1
S	3.4886	3.3789	3.0534	4.3005	4.5835	4.5622	4.2099	3.3471	3.4305	3.4535	3.1650	-4.1	1.5	3.7	-22.2	-25.2	-24.3	-24.8
Cl	0.1169	0.0874	0.1432	0.1391	0.0758	0.1590	0.0709	0.1037	0.0568	0.0941	0.0799	-11.3	-35.0	-44.2	-25.4	-25.0	-40.8	12.6
K	0.5517	0.5858	0.4892	0.4678	0.5080	0.5631	0.4551	0.3064	0.3281	0.3828	0.2780	-44.5	-44.0	-43.2	-34.5	-35.4	-32.0	-38.9
Ca	0.1705	0.1262	0.1024	0.1082	0.0896	0.0891	0.0652	0.1102	0.0729	0.0738	0.0626	-35.4	-42.2	-38.9	1.9	-18.6	-17.1	-4.0
Ti	0.0092	0.0088	0.0079	0.0109	0.0102	0.0114	0.0062	0.0109	0.0084	0.0097	0.0062	18.4	-3.8	-21.4	0.4	-16.9	-15.2	0.5
V	0.0134	0.0137	0.0117	0.0190	0.0237	0.0195	0.0167	0.0175	0.0182	0.0144	0.0177	30.9	32.6	51.3	-7.6	-23.0	-25.9	5.8
Cr	0.0010	0.0009	0.0006	0.0017	0.0015	0.0017	0.0014	0.0014	0.0012	0.0016	0.0011	37.5	35.9	76.3	-16.0	-17.9	-8.0	-17.2
Mn	0.0128	0.0124	0.0077	0.0170	0.0158	0.0170	0.0123	0.0127	0.0113	0.0127	0.0087	-1.0	-8.9	13.0	-25.5	-28.6	-25.2	-28.9
Fe	0.2692	0.1871	0.1219	0.2579	0.1858	0.1996	0.1190	0.2343	0.1325	0.1552	0.0947	-13.0	-29.2	-22.3	-9.2	-28.7	-22.2	-20.5
Co	0.0001	0.0001	0.0002	0.0001	0.0001	0.0001	0.0002	0.0002	0.0002	0.0001	0.0002	21.2	15.1	-26.6	179.5	142.2	12.0	-12.1
Ni	0.0055	0.0054	0.0047	0.0061	0.0071	0.0068	0.0050	0.0049	0.0052	0.0044	0.0050	-11.4	-2.1	6.2	-19.3	-25.9	-34.6	0.1
Cu	0.0113	0.0090	0.0052	0.0110	0.0104	0.0113	0.0065	0.0210	0.0188	0.0167	0.0169	85.3	109.3	226.1	90.8	80.2	48.5	160.5
Zn	0.1794	0.1743	0.1087	0.2399	0.2186	0.2381	0.1727	0.1579	0.1343	0.1600	0.1177	-12.0	-23.0	8.3	-34.2	-38.6	-32.8	-31.9
Ga	0.0004	0.0004	0.0005	0.0018	0.0030	0.0024	0.0026	0.0003	0.0004	0.0003	0.0004	-30.0	-6.8	-16.1	-84.2	-86.8	-88.2	-84.9
As	0.0046	0.0055	0.0042	0.0053	0.0063	0.0084	0.0043	0.0012	0.0010	0.0016	0.0006	-73.6	-82.0	-84.8	-77.0	-84.4	-80.7	-85.1
Se	0.0021	0.0022	0.0020	0.0003	0.0004	0.0005	0.0004	0.0003	0.0004	0.0004	0.0006	-84.7	-83.1	-71.5	-9.4	-4.5	-15.5	33.4
Br	0.0129	0.0127	0.0121	0.0106	0.0099	0.0116	0.0108	0.0172	0.0148	0.0143	0.0174	32.8	17.2	44.6	62.6	49.6	23.3	61.1
Rb	0.0036	0.0043	0.0032	0.0020	0.0025	0.0029	0.0019	0.0010	0.0011	0.0015	0.0008	-72.1	-73.8	-74.4	-49.6	-55.7	-48.7	-56.8
Sr	0.0013	0.0011	0.0011	0.0011	0.0011	0.0015	0.0015	0.0017	0.0019	0.0020	0.0015	33.3	67.8	29.5	51.4	75.4	28.5	1.9
Y	0.0001	0.0001	0.0002	0.0004	0.0004	0.0004	0.0003	0.0003	0.0004	0.0003	0.0004	509.6	195.3	147.4	-24.1	-5.2	-14.7	22.2
Zr	0.0006	0.0006	0.0005	0.0016	0.0013	0.0007	0.0010	0.0010	0.0008	0.0011	0.0010	77.3	41.1	86.1	-33.0	-36.5	55.9	-3.5
Mo	0.0005	0.0005	0.0007	0.0015	0.0011	0.0017	0.0012	0.0007	0.0006	0.0007	0.0005	28.1	16.9	-19.8	-53.1	-42.9	-55.7	-54.0
Pd	0.0012	0.0017	0.0011	0.0019	0.0014	0.0016	0.0020	0.0006	0.0007	0.0008	0.0005	-54.0	-57.6	-58.7	-70.5	-47.5	-52.8	-76.0
Ag	0.0011	0.0017	0.0014	0.0013	0.0020	0.0018	0.0012	0.0010	0.0007	0.0008	0.0007	-9.8	-60.3	-49.7	-28.3	-66.8	-58.9	-37.5
Cd	0.0019	0.0023	0.0022	0.0022	0.0021	0.0025	0.0018	0.0008	0.0007	0.0007	0.0005	-60.3	-70.3	-79.7	-65.7	-67.9	-72.9	-74.8
In	0.0018	0.0020	0.0014	0.0009	0.0010	0.0017	0.0011	0.0005	0.0005	0.0005	0.0005	-74.6	-73.2	-67.0	-48.6	-45.2	-68.3	-59.2
Sn	0.0188	0.0203	0.0116	0.0131	0.0118	0.0162	0.0084	0.0107	0.0101	0.0100	0.0091	-43.1	-50.0	-21.3	-18.4	-13.9	-38.4	9.2
Sb	0.0046	0.0049	0.0038	0.0042	0.0027	0.0039	0.0033	0.0009	0.0009	0.0014	0.0015	-80.8	-81.9	-60.9	-78.8	-66.8	-63.8	-55.8
Ba	0.0267	0.0170	0.0089	0.0106	0.0081	0.0068	0.0053	0.0031	0.0031	0.0024	0.0026	-88.5	-81.5	-70.3	-71.1	-61.5	-64.6	-49.7
La	0.0131	0.0087	0.0130	0.0105	0.0081	0.0082	0.0112	0.0036	0.0034	0.0040	0.0053	-72.2	-60.9	-59.1	-65.5	-57.8	-50.7	-52.6
Au	0.0003	0.0005	0.0004	0.0003	0.0006	0.0002	0.0003	0.0000	0.0000	0.0001	0.0002	-86.3	-90.3	-56.2	-85.4	-93.1	-57.5	-30.0
Hg	0.0001	0.0002	0.0001	0.0000	0.0003	0.0001	0.0001	0.0000	0.0000	0.0000	0.0000	-85.8	-96.8	-93.8	-65.5	-98.2	-100.0	-93.3
Tl	0.0001	0.0001	0.0001	0.0002	0.0001	0.0000	0.0003	0.0000	0.0001	0.0001	0.0000	-45.7	-44.2	-77.8	-77.5	-20.9	298.1	-90.0
Pb	0.0664	0.0726	0.0576	0.0478	0.0498	0.0624	0.0432	0.0405	0.0406	0.0437	0.0399	-39.0	-44.1	-30.7	-15.2	-18.4	-30.0	-7.6
U	0.0002	0.0002	0.0002	0.0013	0.0011	0.0017	0.0018	0.0008	0.0007	0.0007	0.0010	266.5	277.9	534.4	-39.9	-38.1	-61.1	-47.0

5 SUMMARY AND RECOMMENDATIONS

Between 12/06/2008 and 12/29/2009, chemically speciated $PM_{2.5}$ was measured every sixth day in Hong Kong at four sites representing air quality at roadside, urban, and rural areas. A total of 66, 67, 68, and 63 samples were collected from the Mong Kok (MK), Tsuen Wan (TW), Yuen Long (YL), and Hok Tsui (HT) sites. The highest annual (1/5/2009 – 12/29/2009) mean $PM_{2.5}$ mass of ~41.6 μg m^{-3} was found at the roadside MK site. The lowest annual mean of ~24.1 μg m^{-3} was found at the rural HT site, but this value is still much higher than the U.S. EPA annual 24-hr $PM_{2.5}$ standard of 15 μg m^{-3}.

Data was validated through various comparisons between different measurements. Reconstructed mass and measured mass were highly correlated with R^2 = 0.98–0.99, which further supported the validity of gravimetric and chemical measurements. On average, the reconstructed mass explained ~90% of the measured $PM_{2.5}$. The sulfate levels on filter blanks were higher and more variable than those in earlier years, suggesting a potential contamination for the current batches of QMA filters. This is supported by relatively high sulfate/sulfur mass ratios (3.2–3.4). The sulfate contamination was likely in the form of sodium and/or potassium sulfate, and so high blank soluble sodium and potassium levels were also observed. The contamination is not likely to influence the average and high sulfate concentrations significantly, but low sulfate concentrations might be biased high in terms of percentage. It should be noted that the LQL for water-soluble sulfate, sodium, and potassium is 1.4, 2.2, and 0.095 μg m^{-3}, respectively, and is ~13, 750, and 31% of the respective average ambient concentration. Since field blank of sulfate was highly variable, it was not subtracted from ambient concentrations. Mean sulfate concentration may therefore be overestimated by up to 13%.

Sulfate contributed pretty equally across the four sites (9.7–11.0 μg m^{-3}). Nitrate was significantly lower than sulfate, and the lowest values occurred at the HT site. Ammonium was reasonably balanced by sulfate and nitrate. Contributions of crustal material and trace elements were minor, accounting for <5 % of $PM_{2.5}$ mass and lacking distinct spatial variations. Carbonaceous material still accounted for about half of $PM_{2.5}$ mass at MK, although the OC and EC concentrations had been decreasing since 2001. The EC/OC ratio of >1 at the roadside MK site indicated the substantial influence from diesel-vehicle exhausts.

Monthly average $PM_{2.5}$ concentration and chemical composition are shown in Figure 5.1. Hong Kong experienced higher $PM_{2.5}$ concentrations in winter months, primarily due to elevated ammonium sulfate and ammonium nitrate levels. The two highest sulfate episodes appeared on 1/23/09 and 12/1/09. Since sulfate is linked to regional transport, wind direction plays an important role in ambient sulfate concentrations. Wind direction shifted from northwesterly in winter to southeasterly in summer, bringing in clean marine air that improved air quality in Hong Kong. However, it may take several years of monitoring to establish a statistically significant seasonal and inter-annual variation.

EC concentrations at MK were generally higher than at the other three sites, but no significant seasonal trend was observed (Figure 5.1). OC at MK was generally higher in winter, which led to a lower EC/OC ratio in winter. Whether this is due to aerosol microphysics, secondary aerosol formation, or atmospheric boundary-layer dynamics warrants further investigation. A close comparison of EC concentrations with local meteorological parameters, such as wind speed, wind direction, and boundary-layer mixing

height should provide useful insights. Seasonal trends of EC and OC at TW and YL were similar while at rural HT EC also showed significant summer lows and winter highs.

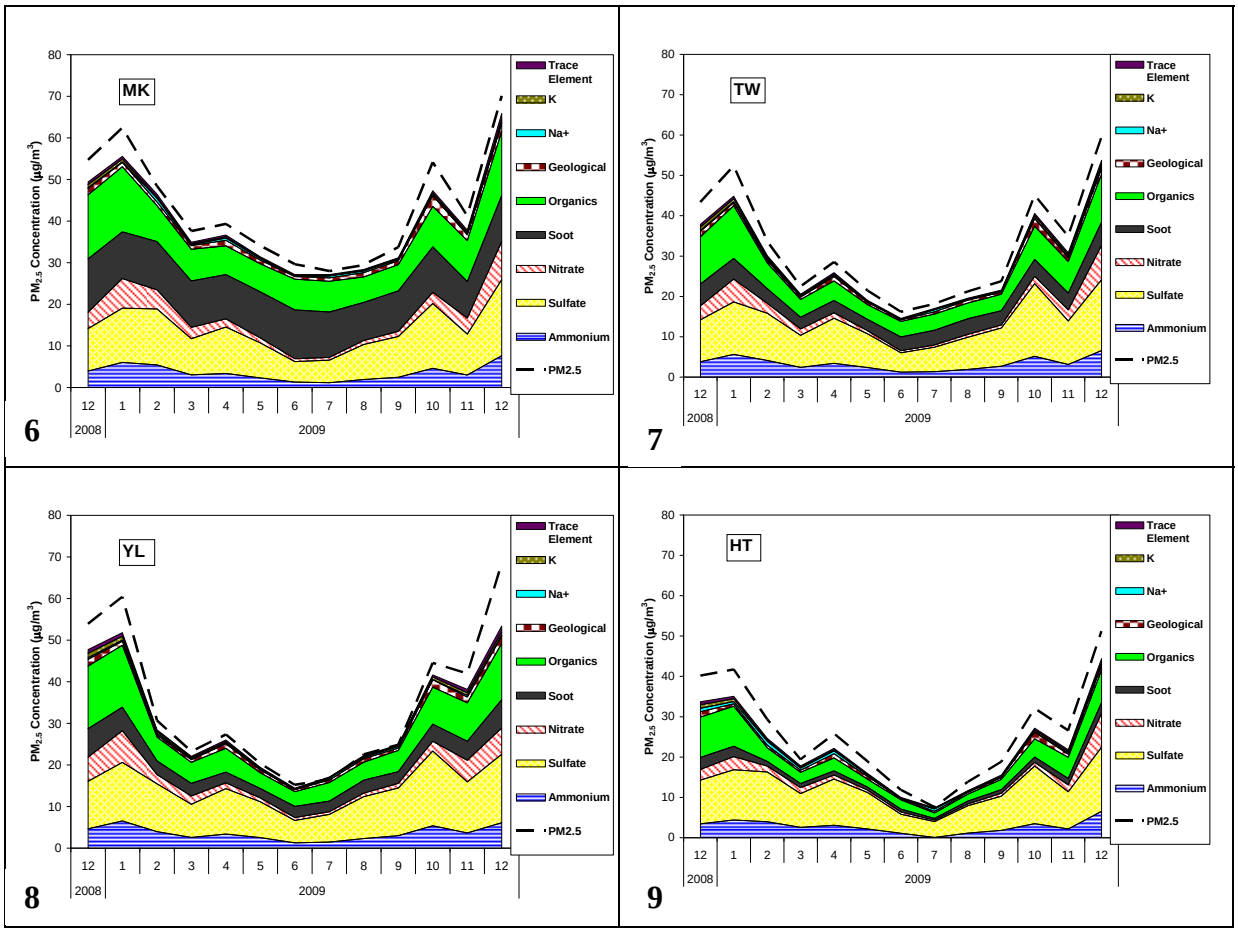

Figure 5-1. Seasonal variation of $PM_{2.5}$ concentration and chemical composition in Hong Kong during the 2008/2009 Particulate Matter Study.

Crustal material concentrations at all four sites were similar and may partially be attributable to long-range transport of fine-mode fugitive dust. There were a few high dust events, including one episode that occurred on 10/20/09 – 10/22/09. At HT, the dust event somehow tracked the TC concentration, and therefore road dust from traffic in the nearby urban areas might also be important. Further data analysis needs to examine the variation of dust composition, such as the Si/Ca ratio to identify the most likely origins.

Variation of $PM_{2.5}$ mass concentrations and their major components over sites and study years were also evaluated. The reduction in $PM_{2.5}$ mass and carbon levels at MK and urban sites indicates an effective control of vehicular emissions over the years which significantly reduce the roadside carbon as well as $PM_{2.5}$ levels. With regard to the variation of secondary pollutants (sulfate, nitrate and ammonium) which are often considered as markers for regional air pollution, a substantial decrease is identified for sulfate and ammonium at all the sites during 2005–2009. Nitrate concentration, however, has been increasing during the same period. The results suggest nitrate substitution when sulfate concentration decreases. Emission control over nitrate precursors, such as reactive nitrogen oxides, need to be evaluated.

Recommendations for future work include:

1. Replace QMA quartz-fiber filters with Pall Life Sciences (Ann Arbor, MI) 47-mm diameter, pre-fired quartz-fiber filters (#2500QAT-UP). These filters were used during the first 12-month study and showed relatively low contamination.
2. Source quantification: This study acquired rich inorganic and organic ambient data. However, better knowledge of local and regional pollution sources is needed in order to understand how emissions are related to ambient concentrations, human exposure, and health effects. Such knowledge can be obtained by measuring source emissions, determining emission profiles, and estimating emission inventories. Similar data from other countries are not necessarily applicable to Hong Kong because of differences in sources and atmospheric transformation.
3. Data analysis: A comprehensive data analysis effort that integrates meteorological and chemical data is very important to implementing effective pollution controls and regulations (e.g., Chen et al., 2010). This may include chemical mass balance analysis (which requires source information) and factor analysis to quantify contributions from all potential sources. Receptor models, such as wind rose and ensemble air parcel back trajectory, are useful for determining source regions and providing a basis for full chemical transport modeling.

6 REFERENCES

Bevington, P.R. (1969). *Data Reduction and Error Analysis for the Physical Sciences*. McGraw Hill, New York, NY.

Chen, L.-W.A.; Chow, J.C.; Watson, J.G.; Moosmüller, H.; and Arnott, W.P. (2004). Modeling reflectance and transmittance of quartz-fiber filter samples containing elemental carbon particles: Implications for thermal/optical analysis. *J. Aerosol Sci.*, **35**(6):765-780.

Chen, L.-W.A.; Watson, J.G.; Chow, J.C.; DuBois, D.; Herschberger, L. (2010). $PM_{2.5}$ source apportionment in Minnesota, USA: Application of the chemical mass balance method to urban and rural monitoring networks. *Atmos. Environ.*, in press.

Chow, J.C. (1995). Critical review: Measurement methods to determine compliance with ambient air quality standards for suspended particles. *J. Air Waste Manage. Assoc.*, **45**(5):320-382.

Chow, J.C.; and Watson, J.G. (1989). Summary of particulate data bases for receptor modeling in the United States. In *Transactions, Receptor Models in Air Resources Management*, J.G. Watson, Ed. Air & Waste Management Association, Pittsburgh, PA, pp. 108-133.

Chow, J.C.; and Watson, J.G. (1992). Fugitive emissions add to air pollution. *Environ. Protect.*, **3**:26-31.

Chow, J.C.; and Watson, J.G. (1994). Contemporary source profiles for geological material and motor vehicle emissions. Report No. DRI 2625.2F. Prepared for U.S. EPA, Office of Air Quality Planning and Standards, Research Triangle Park, NC, by Desert Research Institute, Reno, NV.

Chow, J.C.; and Watson, J.G. (1999). Ion chromatography in elemental analysis of airborne particles. In *Elemental Analysis of Airborne Particles, Vol. 1*, S. Landsberger and M. Creatchman, Eds. Gordon and Breach Science, Amsterdam, pp. 97-137.

Chow, J.C.; Watson, J.G.; Lowenthal, D.H.; Solomon, P.A.; Magliano, K.L.; Ziman, S.D.; and Richards, L.W. (1993a). PM_{10} and $PM_{2.5}$ compositions in California's San Joaquin Valley. *Aerosol Sci. Technol.*, **18**:105-128.

Chow, J.C.; Watson, J.G.; Lu, Z.; Lowenthal, D.H.; Frazier, C.A.; Solomon, P.A.; Thuillier, R.H.; and Magliano, K.L. (1996). Descriptive analysis of $PM_{2.5}$ and PM_{10} at regionally representative locations during SJVAQS/AUSPEX. *Atmos. Environ.*, **30**(12):2079-2112.

Chow, J.C.; Watson, J.G.; Chen, L.-W.A.; Arnott, W.P.; Moosmüller, H.; and Fung, K.K. (2004). Equivalence of elemental carbon by Thermal/Optical Reflectance and Transmittance with different temperature protocols. *Environ. Sci. Technol.*, **38**(16):4414-4422.

Chow, J.C.; Watson, J.G.; Chen, L.-W.A.; Paredes-Miranda, G.; Chang, M.-C.O.; Trimble, D.; Fung, K.K.; Zhang, H.; Yu, J.Z. (2005). Refining temperature measures in thermal/optical carbon analysis. *Atmos. Chem. Phys.*, **5**(4): 2961-2972. 1680-7324/acp/2005-5-2961.

Chow, J.C.; Watson, J.G.; Chen, L.-W.A.; Chang, M.C.O.; Robinson, N.F.; Trimble, D.; Kohl, S.D. (2007). The IMPROVE_A temperature protocol for thermal/optical carbon analysis: Maintaining consistency with a long-term database. *J. Air Waste Manage. Assoc.*, **57**(9): 1014-1023.

Davidson, C.I.; Phalen, R.F.; Solomon, P.A. (2005). Airborne particulate matter and human health: A review. *Aerosol Sci. Technol.*, **39**(8): 737-749.

Fitz, D.R. (1990). Reduction of the positive organic artifact on quartz filters. *Aerosol Sci. Technol.*, **12**(1):142-148.

Green, M.C.; Chow, J.C.; Hecobian, A.; Etyemezian, V.; Kuhns, H.D.; and Watson, J.G. (2002). Las Vegas Valley Visibility and $PM_{2.5}$ Study: Final report. Prepared for Clark County Dept. of Air Quality Management, Las Vegas, NV, by Desert Research Institute, Las Vegas, NV.

Hidy, G.M. (1985). Jekyll Island meeting report: George Hidy reports on the acquisition of reliable atmospheric data. *Environ. Sci. Technol.*, **19**(11):1032-1033.

Lee, K.W.; and Ramamurthi, M. (1993). Filter collection. In *Aerosol Measurement: Principles, Techniques and Applications*, K. Willeke and P.A. Baron, Eds. Van Nostrand, Reinhold, New York, NY, pp. 179-205.

Lioy, P.J.; Watson, J.G.; and Spengler, J.D. (1980). APCA specialty conference workshop on baseline data for inhalable particulate matter. *J. Air Poll. Control Assoc.*, **30**(10):1126-1130.

Lippmann, M. (1989). Sampling aerosols by filtration. In *Air Sampling Instruments for Evaluation of Atmospheric Contaminants*, 7 ed., S.V. Hering, Ed. American Conference of Governmental Industrial Hygienists, Cincinnati, OH, pp. 305-336.

Louie, P.K.K.; Chow, J.C.; Chen, L.-W.A.; Watson, J.G.; Leung, G.; and Sin, D. (2005a). PM2.5 chemical composition in Hong Kong: Urban and regional variations. *Sci. Total Environ.*, **338**(3):267-281.

Louie, P.K.K.; Watson, J.G.; Chow, J.C.; Chen, L.-W.A.; Sin, D.W.M.; and Lau, A.K.H. (2005b). Seasonal characteristics and regional transport of PM2.5 in Hong Kong. *Atmos. Environ.*, **39**(9):1695-1710.

Solomon, P.A.; Klamser, T.; Egeghy, P.; Crumpler, D.; Rice, J. (2004). STN/IMPROVE comparison study - Preliminary results. 10 February 2004.

Subramanian, R.; Khlystov, A.Y.; Robinson, A.L. (2006). Effect of peak inert-mode temperature on elemental carbon measured using thermal-optical analysis. *Aerosol Sci. Technol.*, **40**: 763-780.

Turpin, B.J.; Huntzicker, J.J.; and Hering, S.V. (1994). Investigation of organic aerosol sampling artifacts in the Los Angeles Basin. *Atmos. Environ.*, **28**(19):3061-3071.

Watson, J.G.; and Chow, J.C. (1993). Ambient air sampling. In *Aerosol Measurement: Principles, Techniques and Applications*, K. Willeke and P.A. Baron, Eds. Van Nostrand, Reinhold, New York, NY, pp. 622-639.

Watson, J.G.; and Chow, J.C. (1994). Particle and gas measurements on filters. In *Environmental Sampling for Trace Analysis*, B. Markert, Ed. VCH, New York, pp. 125-161.

Watson, J.G.; Chow, J.C.; and Frazier, C.A. (1999). X-ray fluorescence analysis of ambient air samples. In *Elemental Analysis of Airborne Particles, Vol. 1*, S. Landsberger and M. Creatchman, Eds. Gordon and Breach Science, Amsterdam, pp. 67-96.

Watson, J.G.; Lioy, P.J.; and Mueller, P.K. (1989). The measurement process: Precision, accuracy, and validity. In *Air Sampling Instruments for Evaluation of Atmospheric Contaminants, Seventh Edition*, 7th ed., S.V. Hering, Ed. American Conference of Governmental Industrial Hygienists, Cincinnati, OH, pp. 51-57.

Watson, J.G.; Turpin, B.J.; and Chow, J.C. (2001). The measurement process: Precision, accuracy, and validity. In *Air Sampling Instruments for Evaluation of Atmospheric Contaminants*, *Ninth Edition*, 9th ed., B.S. Cohen and C.S.J. McCammon, Eds. American Conference of Governmental Industrial Hygienists, Cincinnati, OH, pp. 201-216.

Watson, J.G.; Chow, J.C.; Chen, L.-W.A.; Frank, N.H. (2009). Methods to assess carbonaceous aerosol sampling artifacts for IMPROVE and other long-term networks. *J. Air Waste Manage. Assoc.*, **59**(8): 898-911.